X-645-73-226
PREPRINT

NASA TM X-70443

NEAR EARTH MAGNETIC DISTURBANCE IN TOTAL FIELD AT HIGH LATITUDES

II. INTERPRETATION OF DATA FROM OGO'S 2, 4, AND 6

R. A. LANGEL

(NASA-TM-X-70443) NEAR EARTH MAGNETIC DISTURBANCE IN TOTAL FIELD AT HIGH LATITUDES. 2: INTERPRETATION OF DATA FROM OGO'S 2, 4, AND 6 (NASA) 74 p HC $5.75 CSCL 08N G3/13 N73-30332 Unclas 11973

AUGUST 1973

GSFC — GODDARD SPACE FLIGHT CENTER
GREENBELT, MARYLAND

NEAR EARTH MAGNETIC DISTURBANCE IN TOTAL FIELD AT HIGH LATITUDES

II. INTERPRETATION OF DATA FROM OGO'S 2, 4, AND 6

by

R. A. Langel

Laboratory for Space Physics

Goddard Space Flight Center

Greenbelt, Maryland 20771

August 1973

GODDARD SPACE FLIGHT CENTER

Greenbelt, Maryland

NEAR EARTH MAGNETIC DISTURBANCE IN TOTAL FIELD AT HIGH LATITUDES

II. INTERPRETATION OF DATA FROM OGO'S 2, 4, AND 6

by

R. A. Langel

ABSTRACT

Variations in the scalar magnetic field (ΔB) from the polar orbiting OGO 2, 4, and 6 spacecraft, with supporting vector magnetic field data from surface observatories, are analyzed at dipole latitudes above 55°. Data from all degrees of magnetic disturbance are included with emphasis on periods when Kp = 2^- to 3^+. Although individual satellite passes, at low altitudes, confirm the existence of electrojet currents, neither individual satellite passes nor contours of average ΔB are consistent with latitudinally narrow electrojet currents as the principal source of ΔB at the satellite. The total field variations at the satellite form a region of positive ΔB between about 22^h and 10^h MLT and a region of negative ΔB between about 10^h and 22^h MLT. Further characteristics are given by Langel (1973b). The ratio of ΔB magnitudes in these positive and negative regions is variable. The characteristics of the negative ΔB region indicate a latitudinally broad ionospheric source. Equivalent current systems were derived from satellite data in the negative ΔB region for summer, winter, and equinox seasons for Kp = 2^- to 3^+. Comparison of the surface magnetic disturbance caused by the equivalent current with the measured average surface disturbance shows good

Preceding page blank

agreement except in localized details. Because ΔB decreases very slowly with altitude in the positive ΔB region, it is not possible to account for this disturbance in terms of ionospheric currents. The contribution to the satellite ΔB due to a model electrojet, which reproduced the measured average surface horizontal disturbance, was computed. When the contribution to ΔB from this model electrojet is removed from the measured satellite ΔB, the remaining ΔB is constant with altitude within experimental error. This non-electrojet ΔB is estimated to be about 50-80γ, 20-30γ, and 7-15γ, respectively, for $Kp \geqslant 4^-$, 2^- to 3^+, and 1^- to 1^+. It is concluded that most, if not all, of the non-electrojet positive ΔB is extra-ionospheric in origin. Some of this non-ionospheric ΔB is caused by the Equatorial Current Sheet (Ring Current), but some data cannot be accounted for in terms of this source. Definitive identification of all sources of positive ΔB is not possible at this time.

CONTENTS

CONTENTS (continued)

TABLES

ILLUSTRATIONS

NEAR EARTH MAGNETIC DISTURBANCE IN TOTAL FIELD AT HIGH LATITUDES

II. INTERPRETATION OF DATA FROM OGO'S 2, 4, AND 6

INTRODUCTION

This paper is an analysis of high latitude magnetic field data from the Polar Orbiting Geophysical Observatory (POGO) satellites OGO 2, 4, and 6, supplemented by data from magnetic observatories on the earth's surface. "High latitude" is defined as auroral belt and polar cap latitudes (invariant latitudes above about 55°). The POGO magnetometers measured the magnitude, but not the direction, of $\vec{B}$. The quantity analyzed is $\Delta B = |\vec{B}| - |\vec{M}|$, where $\vec{M}$ is a mathematical model of the quiet time field. A summary of the accuracy of $|\vec{B}|$, the characteristics of the field model (denoted POGO(8/71)) used for $\vec{M}$, and the average characteristics of ΔB are given in a companion paper (Langel, 1973b) which will henceforth be denoted paper I.

Paper I describes the average characteristics of ΔB as a function of geomagnetic season, Kp, and altitude. Geomagnetic season was defined relative to the dipole latitude of the sub-solar point, θ_{sun}, namely:

$|\theta_{sun}| < 10°$ is equinox,

$\theta_{sun} > 10°$ is northern summer, and

$\theta_{sun} < -10°$ is northern winter.

Data subdivision by Kp was into four levels: (1) Kp = 0 to 0^+, (2) Kp = 1^- to 1^+, (3) Kp = 2^- to 3^+, and (4) Kp $\geqslant 4^-$. Data division by altitude was into the ranges

<550 km., 550-700 km., 700-900 km., and >900 km. For details regarding the spacecraft and experiment, the data accuracy, and the statistics of the averaging process, the reader should consult paper I and the references therein.

In paper I it was shown that the basic pattern of ΔB is a positive disturbance between 22^h and 10^h MLT (magnetic local time) and a negative disturbance between 10^h and 22^h MLT. These regions were designated the positive ΔB region and the negative ΔB region, respectively. Both regions have broad maxima. In the positive ΔB region the maximum is between 2^h and 5^h MLT, and in the negative ΔB region it is between 14^h and 18^h MLT. Equatorward of approximately 65°, ΔB reverses weakly, i.e., the peak value in the reversed region is usually much less than one fifth the magnitude of the peak value in the poleward region. As an example, Figure 1 shows average ΔB contours in the northern hemisphere for $Kp = 2^-$ to 3^+. These averages are for the usual (geographic) equinox months (summer = May through Aug.; winter = Nov. through Feb.; equinox = Mar., Apr., Sept., Oct.). Comparison with Figure 2 of paper I for geomagnetic equinox shows no substantial differences between the averages for the two definitions of season; this is also true for the other seasons and Kp ranges. The major characteristics of ΔB are noted in paper I and will not be repeated here.

Previous Results from Surface Data

Magnetic disturbance measured at surface observatories are conveniently represented by equivalent current systems (i.e., systems of currents in the E-region ionosphere which would cause the magnetic variations observed on the ground). Two categories of such current systems exist, namely: (1) those systems which contain intense currents confined to about 6° or less in latitudinal extent, flowing along the statistical auroral belts, and (2) those systems in which all dimensions are spatially broad and in which sharp boundaries through which large changes in current magnitude occur are not present. The first category will be referred to as an "electrojet system" or a jet-type current throughout this study. Current closure from the jet-type currents may occur via spatially broad currents.

The dominant magnetic field variations at high latitudes are thought to be due to a system of currents called the "auroral (or polar) electrojet system" which falls into category (1) above. Figure 2 (a combination of a figure from Feldstein, 1969, and one from Sugiura and Heppner, 1972) shows, schematically, four equivalent current systems discussed in the literature in recent years. A feature of all four systems is a high concentration of westward current, the westward electrojet, in the 22^h to 6^h MLT (magnetic local time) region. Three of these systems (a, c, and d) include an eastward electrojet in the evening. Current closure is shown to occur at lower latitudes and over the polar cap. Although closure of actual current flow is probably not confined to the ionosphere (see e.g. Heppner et al., 1971), it is widely believed that electrojet currents (particularly the westward electrojet) do indeed flow in the ionospheric E-region. Those observed features of observatory magnetic data (e.g. Heppner, 1954) which are represented by the equivalent current systems of Figure 2 include: (1) positive variations in H (the horizontal component of the field) in the evening auroral belt ($\sim 19^h$ - 23^h MLT), (2) negative variations in H in the morning auroral belt ($\sim 23^h$ - 6^h MLT), and (3) a horizontal variation approximately directed from 2^h to 14^h MLT across the polar cap. Positive and negative variations in H are called "bays" because the ΔH trace on a magnetogram often resembles a topographic bay. A reversal in ΔZ (the magnetic variation in the vertical direction) occurs in the auroral belt near the latitude of maximum ΔH.

Stagg (1935) noted that the magnitude of high latitude magnetic disturbances is larger in summer months than in winter months. This relationship was investigated by Meng and Akasofu (1968) using the near conjugate pairs of stations College - Macquarie and Reykjavik - Syowa. They found that the ratio of peak magnitudes of positive bays of the summer station to the winter station ranged from 1 to 5 with the average equal to 2. A tendency exists for the ratio to decrease as time progresses from early afternoon to midnight. Ratios for negative bays were closer to one. They concluded that the conductivity in the positive bay region is controlled by solar radiation rather than particle precipitation. Kamide and Fukushima (1972) suggest two types of positive bays: (1) a broad variation in the evening sector which is controlled by ionization due to solar radiation and exhibits a large seasonal change and (2) event-type bays in the nightside auroral region. The event-type bays did not show a seasonal variation.

Fukushima (1962), using individual station K-indices, showed that magnetic disturbance is present in the sunlit polar cap region, even during periods of magnetic quiet at lower latitudes. He noted a large seasonal variation in this polar cap disturbance from 10-20γ in winter to 50-200γ in summer. Further study of quiet time polar cap disturbance was carried out by Nagata and Kokubun (1962), who derived the quiet day current system shown in Figure 3 (a and b). This is an example of a current system with broad spatial dimensions and no electrojet. They also analytically extended the low latitude S_q current system to high latitudes and subtracted it from the current of Figure 3 (a and b). The resulting current system was called S_q^p. In contrast to the current shown in Figure 3 (a and b), Kawasaki and Akasofu (1967) and Feldstein and Zaitzev (1967, 1968) find no disturbance near midnight during quiet intervals; rather the disturbance is confined to the sunlit portion of the polar cap. The resulting single vortex current system of Feldstein and Zaitzev, called DPC, is shown in Figure 3c.

Nishida and co-workers (1966) noted that certain fluctuations in polar cap and equatorial magnetic field occur in-phase. Analysis of such data (see also Nishida, 1968a, b, 1971; Nishida and Maezawa, 1971) led these workers to identify these disturbances with S_q^p, except that they noted that the disturbance is worldwide and not confined to the polar regions. An example of the current system, called DP2 or SP, derived by Nishida and co-workers is given in Figure 3 (d and e).

Noting that the seasonal change in S_q^p is very much like the seasonal change in positive bay intensity found by Meng and Akasofu (1968), Kokubun (1971) suggests that the eastward current causing positive bays is more like S_q^p than like a jet-type current, i.e., broad in latitudinal extent rather than jet-like, and conductivity controlled by solar radiation rather than particle precipitation.

Features of the Present Study

Although other "types" of magnetic variation do occur at high latitudes, those due to the electrojet system are predominant. Transverse ionospheric conductivities above the E-region are small (both electrons and protons move essentially with an $\vec{E} \times \vec{B}$ drift), and magnetospheric currents (ring current, tail current, magnetopause currents) are at large distances from the low orbiting (400 - 1510 km.) POGO. Because POGO is much closer to the E-region than to other known sources, and because of the dominance of the electrojet system in the observatory data, it was expected that the main cause of ΔB at the POGO would be the electrojet system. This study, however, will show that the principal source for ΔB at the POGO cannot be a jet-type current.

With the exceptions of some rocket-borne magnetic field measurements and a limited number of single component transverse magnetic field measurements from satellite, previous studies of high latitude magnetic fields have utilized data only at the earth's surface. The POGO data makes it possible to study average magnetic field characteristics as a function of altitude. Knowledge of the altitude dependence of magnetic variations enables us to demonstrate that certain magnetic variations are ionospheric in origin while others are not. Additional features of the data include: (1) the possibility of direct comparison of POGO data above the ionospheric E-region with observatory data below the ionosphere as the satellite passes over individual observatories, and (2) the ability to obtain a closely spaced latitude profile across the auroral belt in about 5 minutes, a time short enough so that most of the measured magnetic variations are spatial rather than temporal.

Although a unique resolution of the measured disturbance into portions due to individual sources is not attainable, it is possible to show some of the major characteristics of the sources which produce a ΔB variation at POGO altitudes. In particular, we will show that: (1) the source of ΔB at sunlit local times, particularly from about 10^h to 18^h MLT, is an ionospheric current with characteristics similar to those of the DPC current system proposed by Feldstein and co-workers (Figure 3c) for quiet summer days, and with seasonal properties similar to those found for these MLT by Stagg (1935), Fukushima (1962), Negata and Kokubun (1962), and Meng and Akasofu (1968), and (2) the dominant source of ΔB from 21^h to 9^h MLT is not ionospheric in origin, although the westward electrojet does contribute. ΔB from both the eastward and westward electrojets is apparent in the low altitude POGO data, and such data will be discussed in a subsequent paper, but these sources are not the main contributors to ΔB.

GENERATION OF EQUIVALENT CURRENTS

It was shown in paper I that $\Delta Z \doteq \Delta B$ is a good approximation at the latitudes considered. Using this assumption, it is possible to compute a potential, Ve, which represents the disturbance field at satellite altitudes. The assumption $\Delta B \doteq \Delta Z$ is tested by computing the vector disturbance from Ve and comparing the resulting ΔB and ΔZ. As will be shown, ΔZ and ΔB from this computation are nearly equal, which gives justification to the procedure. If a further assumption is made that the source currents for the field described by Ve flow at 115 km., it is possible to derive a current function, ψ, which describes the required currents, and a potential function, Vi, which describes the disturbance due to the currents, ψ, at altitudes below 115 km. In particular, Vi can be used to compute the vector disturbance field due to ψ at the earth's surface.

Determinations of the disturbance functions Ve, Vi, and ψ were carried out for each season and for all Kp ranges. Comparison of the altitude dependence of the measured ΔB and the ΔB predicted by Ve showed that the altitude variation in the positive ΔB region could not be reproduced by this type of current system for any season and Kp range. For example, Figure 4 shows the altitude variation of the contours of maximum disturbance from both the average data and for the field from Ve for the (geographic) equinox and summer months for Kp = 2^- to 3^+. The computed altitude variation in the positive ΔB region falls off far more rapidly with altitude than does the measured altitude variation. In the negative ΔB region the altitude variation is reproduced in a reasonable fashion. The inability to reproduce ΔB in the positive ΔB region is not surprising in view of the small decrease in ΔB with altitude discussed in paper I.

Another shortcoming of the derived current system in the positive ΔB region is that the resulting disturbance at the earth's surface largely disagrees with the measured average disturbance (Langel, 1973a) at the earth's surface.

It is concluded that the positive ΔB region cannot be accounted for by a current system of the type derived here because of a breakdown of the assumption that all currents are located below satellite altitudes.

EQUIVALENT IONOSPHERIC CURRENTS AS SOURCES FOR THE NEGATIVE ΔB REGION

As the altitude variation of ΔB from the derived potential function is in agreement with the measured altitude variation in the negative ΔB region, current systems are derived for this region only. Contours computed from the resulting Ve for months 3, 4, 9 and 10 for $Kp = 2^{-}$ to 3^{+} are shown in Figure 5. ΔB is given by the solid contours, and ΔZ is given by the dashed contours. Comparison indicates that ΔZ and ΔB are close enough to give confidence in the procedure used.

Figure 5 is to be compared with the measured negative ΔB regions in Figure 1. Computed contours for months 11, 12, 1, 2 and for months 5, 6, 7, 8 have also been compared with the corresponding measured data. In all cases the major features of the computed contours are in good agreement with the major features of the measured contours. In particular, measured and computed amplitude levels at all altitudes are generally within 5γ, which is as close as would be expected considering the uncertainties in the data and the assumptions in the determination of Ve.

Figure 6 shows contours of the current functions derived for each season and drawn so that 10^4 amps flows between contour lines. Arrows on certain flow lines indicate current direction. The current patterns in Figure 6 are quite similar to DPC and to the dayside vortices of S_q^p and DP2 (Figure 3). The current systems derived in this chapter will be denoted as HLS (High Latitude, Sunlit) for convenience of discussion.

Comparison of the Surface Disturbance from HLS to the Measured Surface Disturbance

A test of the reality of HLS is to compare the surface disturbance which HLS would cause to the measured surface disturbance. Langel (1973a) published average surface disturbance patterns for the same Kp ranges and geomagnetic seasons for which average satellite ΔB patterns have been computed for the POGO data. The surface data was also subdivided by interplanetary magnetic sector. Differences in ΔB between interplanetary magnetic sectors do occur in the POGO data and will be discussed in a subsequent paper. In this section the computed surface disturbance from HLS for summer, Kp = 2^- to 3^+, for both Away and Toward interplanetary magnetic sectors, is compared with the corresponding measured average surface data from Langel (1973a).

The computed ΔZ is shown in Figure 7 and the computed vector horizontal field is shown in the bottom portions of Figures 9 and 10. The actual average surface disturbance (from Langel, 1973a), which did not enter the computation determining ψ and Vi, is shown in the top portions of Figures 8, 9, and 10. Comparing first Figure 7 with Figure 8, results for the Toward sector are remarkably similar for MLT 12^h to 18^h. The major differences are that the maximum contour of the measured data is -160γ, while that of the computed curve is -130γ; and, the measured maximum is near 14^h, whereas the computed maximum is near 16^h. The correspondence of the lower latitude positive ΔZ is even closer. The separate disturbance peak near 20^h from the measured data is not evident on the computed curve.

For Away sectors the correspondence is not as good. Two maxima near -100γ are evident in the measured data near 11^h and 16^h, while one maximum of greater than -140γ near 15-16^h is evident in the computed curve, which accurately reflects the measured ΔB at the satellites. Langel (1973a) noted that the surface disturbance near 11^h was consistent with a more localized current. The disturbance at satellite altitude from such a current would decrease in amplitude more rapidly with distance than would the disturbance from a more widespread current. Furthermore, as the vertical distance from the "two" sources (i.e., spatially broad current near 16^h and spatially limited current near 11-12^h) increases to a distance comparable with their horizontal separation, the integration of disturbance from the two sources will cause the combined disturbance to merge into one peak. In view of this effect and the small spatial extent of the dayside peak in the measured data, the calculated result is considered to be in fair agreement with the measured data.

Comparison of the measured horizontal disturbance with the computed disturbance in Figures 9 and 10 shows a remarkable similarity both in direction and magnitude. From 16^h to 20^h the magnitude of positive bays is greater for

Toward than Away sectors for both the measured data and the disturbance due to the HLS currents. Directions are comparable except near 14-16^h and 80°-84° for Away sectors, where the measured vectors are directed toward the west or south and the computed vectors are directed toward the east. These measured vectors are one of the evidences for the localized current near 11^h (Langel, 1973a) which would not be detected in ΔB at the altitude of the POGO. Note also that the Y component of the computed vectors in the positive bay region is in the same direction as the measured Y component, except near 70° between 12^h and 14^h.

The horizontal disturbance magnitude on the dawn side of the polar cap is considerably smaller for the computed vectors than for the measured vectors because the current associated with the positive ΔB region or the westward electrojet has not been included.

It should be emphasized that HLS is an equivalent current system. High conductivity gradients between the nightside and sunlit polar cap and at the edges of regions of ionizing particle precipitation make it unlikely that the actual current flow in these regions is as smooth as HLS. Because of the agreement with surface data, however, it is concluded that, with necessary modification to account for gradients in electric field and conductivity, and the resulting magnetic field aligned currents, a current system with characteristics similar to HLS is a common feature of the ionosphere and can account for both the negative ΔB region in the POGO data and for the average characteristics of positive bays at the earth's surface from about 12-18^h MLT.

The Direction of Ionospheric Current Over the Polar Cap

Most equivalent current systems derived from observatory data show current flow approximately directed from 20^h to 8^h MLT across the polar cap (see, e.g., Figure 2). Electric field measurements using barium clouds (Heppner et al., 1971) have indicated that nightside polar cap electric fields are directed nearly dawn to dusk. Such an electric field would result in a Hall current directed from 0^h to 12^h and a Pedersen current directed from dawn to dusk. No combination of currents in these directions can result in a current directed from 20^h to 8^h. (Surface magnetic field disturbance during the time when the barium measurements were made were roughly consistent with a 20^h to 8^h overhead current direction, which could not have resulted from the measured electric field direction.) The direction of the HLS current over the polar cap (Figure 6) is more nearly midnight to noon than previous equivalent current systems, but still seems to be in some disagreement with the electric field directions. These HLS directions, derived only from POGO magnetic field data, are in good agreement with the average surface data, which confirms the current flow direction. Heppner et al., (1971) proposed a solution to this directional discrepancy based on the distribution of field aligned currents. As will be shown, however, such currents do not seem to be able to cause a horizontal magnetic disturbance of the required amplitude.

Because real current flow in the dark portion of the polar cap may be different from HLS (see the discussion of conductivity gradients in the previous section), and because the electric field measurements cited are limited in local time (to the nightside, near twilight) and latitude, the extent of the discrepancy is not presently known. Recent average electric potential patterns derived by Bohse and Aggson (1973) are skewed from noon-midnight in a direction more consistent with the magnetic field data. These patterns, however, have a large degree of uncertainty and so are not conclusive. Maynard (personal communication) has recently measured the perpendicular electric field in the polar cap near noon with a rocket-borne instrument. In this instance, the electric field was directed roughly from $4^h\ 30^{min}$ to $16^h\ 30^{min}$ MLT, which more closely agrees with the magnetic data than does the barium results. A discrepancy of about 20° exists between the electric field at the rocket and the direction of the overhead Hall current required to produce the measured surface magnetic disturbance below the rocket. The existence of an overhead Pedersen current would widen the discrepency. Final resolution of this problem will have to await extensive vector electric field measurements and vector magnetic field measurements from low altitude satellites.

SEPARATION OF POSITIVE ΔB SOURCES

A Numerical Model Electrojet Current which Reproduces the Average Surface Horizontal Disturbance

For this discussion it is assumed that a westward electrojet does exist in the ionospheric E-region at 22^h to $6\text{-}10^h$ MLT, and that an eastward electrojet exists from about 15^h to 22^h MLT. While both of these currents will contribute to ΔB at the POGO, the analysis shows that:

1. The contribution due to the eastward electrojet is negligible except at extremely low altitudes,
2. the contribution due to the westward electrojet is important, but not dominant.

In particular, the field variations in the positive ΔB region consist of an altitude dependent contribution from the westward electrojet and a contribution from another (unspecified) source(s) which results in a ΔB with amplitude relatively constant with altitude.

To test this hypothesis several numerical model electrojet systems have been constructed which reproduce the main features of the average horizontal disturbance at the earth's surface. In particular, the surface data from Langel (1973a) were used as a guide in the construction of most of these models. Heppner et al. (1971) have suggested that, on the average, the electrojet currents may be closed via field aligned currents flowing into the ionosphere in the 7^h to 13^h MLT sector and out of the ionosphere in the 19^h - 1^h MLT sector (near the Harang discontinuity). This suggestion was followed in the construction of the models, with some modifications in order to reproduce the measured averages. In particular, in our models the field aligned currents flow into the ionosphere near 6^h - 10^h MLT and near 13^h - 15^h MLT and out of the ionosphere near 21^h to 1^h MLT.

The finite conductivity of the earth implies that a changing ionospheric current will induce a current within the earth. One technique which has been utilized in constructing models to fit experimental data is to represent the field, external to the earth, due to the induced current by the field due to an image current within the earth. The intensity and depth of the image current are chosen so that the combined fields of the image current and the (primary) ionospheric current reproduce the measured field (e.g. Forbush and Casaverde, 1961; Scrase, 1967). This is the method utilized in the models described in the present study. By varying the current strength in the ionosphere, and the current strength and depth of the induced currents in our models (within reasonable limits), it is possible to hold ΔH nearly constant while varying ΔZ by about 30-50% (at the earth's surface). Comparison of the contributions of the field aligned and ionospheric portions of the current systems indicated that, except in the immediate vicinity of the field aligned currents, the major contribution ($\geq$ 80%) of the resulting fields is due to the ionospheric portion. Because the contribution of the induced currents corresponding to the field aligned current segments is still smaller than the contribution from the primary field aligned segments, this portion of the induced current was omitted so as to increase the speed of computation.

Uncertainties in the parameters of the induced current, the correct average configuration of field aligned current, and the amount of current over the polar cap, limit the value of these models. It is possible, however, to make a semi-quantitative estimate of the effect of electrojet-type currents on the satellite data. The existence of a westward electrojet in the ionospheric E-region is regarded to be established, which implies that the estimate of the effects of this current at satellite altitudes approximates a real contribution to the measured ΔB.

A series of models have been constructed, with variations in current distribution and in the strength of the induced currents, which approximate the measured horizontal disturbance at the earth's surface derived by Langel (1973a) for $Kp = 2^-$ to 3^+ during equinox. As an example, Figure 11 (top) shows contours of ΔZ and the horizontal vector disturbance at the earth's surface from one of these models. On comparison with the measured data we note:

(1) The computed positive Y component in the negative bay region is in the correct direction, although not quite of the right magnitude, to match the measured data. This direction results from the model current moving from higher latitudes to lower latitudes from the dayside to the nightside <u>and</u> from the distribution of field aligned current.

(2) The positive Y component in the positive bay region does not agree with the measured data. (In this connection attention is called to the agreement in Y direction between the measured data and the $\Delta\vec{H}$ from the HLS currents in Figures 9 and 10.)

(3) The polar cap horizontal disturbance is in the same direction as the measured data but is of much smaller magnitude.

(4) ΔZ to the south of the electrojets is not in bad disagreement with the measured data, but the ΔZ to the north of the electrojets is of considerably smaller magnitude than that measured.

The characteristics of these models thus indicate that:

(1) This field aligned current distribution cannot account for the measured horizontal disturbance over the polar cap. This does not rule out the possibility that some other distribution of field aligned and ionospheric current can account for the measured fields. However, the variety of current configurations for which calculations have been performed is sufficient to conclude that systems wherein the field aligned current is restricted to flow into and out of the region of electrojet current are unlikely to account for the measured fields in the polar cap.

(2) Both surface and satellite magnetic disturbance between about 12^h and 19^h are due to a current with characteristics like HLS rather than a jet-type current.

(3) ΔZ at the surface between 0^h and 10^h is not consistent with the westward electrojet as the sole source of disturbance.

Characteristics of ΔB at Satellite Altitude due to the Ionospheric Electrojet

Major characteristics of the ΔB at POGO altitudes due to the electrojet can be found from our numerical models. Figure 11 (bottom) illustrates the results from one model. Major features of importance are:

(1) The contribution to satellite ΔB from the eastward electrojet is small in both cases. (At 453 km on Figure 11 a 5γ contour, not shown, occurs equatorward of the negative ΔB near 18^h.)

(2) ΔB from the westward electrojet is very small at 800 km. (At 815 km. on Figure 11 a -5γ contour, not shown, occurs equatorward of the positive ΔB near 3^h.)

(3) From the westward electrojet, ΔB near 500 km. has both positive and negative peaks whose magnitude ratio is about 2/1.

(4) Comparison of the two altitudes indicates that $|\Delta B|$ drops off rapidly with altitude.

The measured ΔB of Figure 1 and the ΔB due to the model electrojet shown in Figure 11 are for the same season and magnetic disturbance level. Comparison indicates a great contrast both in magnitude and in ΔB distribution. The positive ΔB due to the westward electrojet is about 1/2 and 1/4 the magnitude of the measured positive ΔB at 453 km. and 815 km., respectively, and the magnitude difference is even greater in the negative ΔB region. Differences of this magnitude are not likely to be the result of deficiencies in the numerical model. The contrast in ΔB distribution is seen by noting that the N-S ratio of ΔB magnitude at 453 km is about 2/1 for the model electrojet and about 10/1 for the measured data. It is clear that, on the average, jet-type currents are not the primary source for either the positive or negative ΔB regions.

Remaining ΔB when the Contribution from the Electrojet is Removed

To estimate the ΔB not attributed to the westward electrojet, the ΔB computed from each model electrojet, denoted ΔB_c, has been subtracted from the average ΔB measured by the POGO, denoted ΔB_m, to get $\Delta B'$ $(=\Delta B_m - \Delta B_c)$.

(This subtraction is physically meaningful where $\Delta B \approx \Delta Z$.) Contours of maximum disturbance were determined for $\Delta B'$. In all cases the altitude variation of $\Delta B'$ is reduced considerably from that of ΔB_m, but uncertainties in the models and in ΔB_m do not allow us to determine the actual altitude variation of the ΔB from non-electrojet sources. This disturbance could decrease very slowly with altitude or be constant with altitude. It is also possible to construct a model electrojet such that $\Delta B'$ increases slightly in magnitude with increasing altitude.

<u>Surface ΔZ When the Non-Electrojet Contribution is Removed</u>

Removal of the estimated ΔB contribution attributed to a westward electrojet from the measured ΔB leaves a ΔB which is approximately constant in altitude. This implies that ΔZ measured at the earth's surface is also caused by more than one source. If, then, an estimate of the altitude independent ΔZ is subtracted from the measured ΔZ, the remaining ΔZ should approximate the ΔZ due to the westward electrojet. This should resemble Figure 11 (top right).

The satellite ΔB for 700-900 km. subdivided by interplanetary magnetic sector is utilized as an estimate of the "constant altitude" ΔZ (= ΔB). This ΔB was subtracted from the measured ΔZ for both interplanetary magnetic sectors, and the modified ΔZ, presumably approximating the ΔZ caused by the average westward electrojet, is shown in Figure 12. Comparison with Figure 11 (top right) indicates that the modified ΔZ is in much better agreement with the numerical model than is the original average ΔZ shown in Figure 8 (bottom). This confirms the interpretation of source distribution.

EXAMPLES OF ΔB FROM INDIVIDUAL SATELLITE PASSES

Because average data alone may be misleading, we shall study the variation of ΔB along individual satellite tracks, including a detailed comparison with measurements from observatories close to the satellite path. Data examples are selected to illustrate the following points:

(1) The major source of ΔB at satellite altitude is not a jet-type current.

(2) Between about 12^h and 19^h MLT, in the negative ΔB region, both the surface disturbance and the satellite ΔB are consistent with the HLS current system as the source.

Figure 11 (bottom) illustrates the characteristics of ΔB due to jet-type currents. In particular the ratio of $|\Delta B|$ to the north and south of the locus of zero ΔB is about 2/1. This ratio (2/1) should be regarded as an upper bound because currents in individual disturbance events, as opposed to the averages matched by the models, are likely to have a smaller latitudinal extent or to be more localized in longitude (corresponding to bays observed only in certain regions of the auroral belt).

The Positive ΔB Region

An example from the positive ΔB region at midnight-early morning MLT is shown in Figure 13. The thin line indicates the satellite path and is used as the $\Delta B = 0$ axis. The scale for ΔB is given by the short lines normal to the baseline which project away from the baseline in the direction of positive ΔB. Labels on the scale lines indicate the scale, and the altitude and universal time when the satellite was at the position where the scale line meets the baseline. The time for a complete crossing (from 50° to 50° latitude) is approximately 20 minutes.

In Figure 13, ΔB is positive ($\geqslant 100\gamma$) over a large portion of the polar cap crossing and over the nightside auroral belt, with a peak of nearly 150γ. The magnitude of ΔB is relatively constant over a large portion of the region measured, a not uncommon occurrence. Several observatories are favorably situated for comparison with the POGO data in and near the auroral belt in the night sector. A negative bay with $\Delta H \approx -400\gamma$ at SO (Sodankyla, Table 1 gives a list of observatory mnemonics and positions), positive ΔZ at SO, and negative ΔZ at DO indicate the presence of a westward electrojet with most of the current located just to the south of SO but to the north of DO (the electrojet is presumably located near the latitude of maximum $|\Delta H|$ and zero ΔZ). We particularly note the negative ΔZ at DO, at LO, and even as far south as RS. At the satellite, however, ΔB is always positive, in contrast to the variation expected from an electrojet. In particular, near DO the satellite ΔB is $+30\gamma$ while the surface ΔZ is $\leqslant -100\gamma$. Furthermore, in the numerical models, a peak ΔB of 150γ at an altitude above 800km, from an electrojet, would require a surface $|\Delta H|$ in excess of 1500γ, which is definitely not the case.

A line or ribbon of current near SO should result in a positive ΔB several degrees to the north of SO in the region where the peak of the measured ΔB is located. The interpretation is that at least two sources are present:

(1) a source which causes a relatively constant positive ΔB over much of the polar cap and nightside auroral belt, and

(2) the westward electrojet which causes a peak in positive ΔB near 72° and which decreases ΔB at latitudes near 64°.

The Negative ΔB Region

A principal result of our study is that the source for the negative ΔB region and for positive bays between about 12^h and 18-19^h MLT (i.e., sunlit times) is a current in the ionosphere similar to HLS. Individual pass data are consistent with this interpretation but not with the notion of a jet-type current source. All of the negative ΔB region data shown in this section occurs in that portion of the polar cap which is sunlit. It is the usual case for negative ΔB to occur at sunlit local times after noon, with exceptions near 20-23^h at low altitudes where negative ΔB is due to the eastward electrojet.

The characteristics of the peaks of the ΔB variation are different for HLS and for jet-type currents, and this difference is the important quantity used to distinguish between the two types of sources. As already noted, at about 500km. the ratio of peak $|\Delta B|$ to the north and south of a jet-type current is at most about 2/1. From Figure 5, the corresponding ratio for HLS is more nearly 7/1 and possibly higher, i.e., the lower latitude $|\Delta B|$ is almost an order of magnitude less than the higher latitude $|\Delta B|$. The HLS currents also result in a positive bay magnitude (at the surface) of the same order of magnitude as the peak disturbance of negative ΔB at about 480km., and a peak surface ΔZ which is generally slightly larger in magnitude (factor of 1.1-1.6) than the satellite ΔB near the peak of negative ΔB (again at 480km).

Two passes which illustrate the major features of the negative ΔB region are shown in Figures 14-15. In each case the satellite is at a low altitude (< 520 km.) during passage over the negative ΔB region, and both passes are at nearly identical local times. Although the magnitude, location, and extent of the negative ΔB varies considerably, both passes have the common feature that $|\Delta B|$ to the north of FC is much larger ($\geqslant 6/1$) than that to the south of FC. This fact alone eliminates a jet-type current as the major source of disturbance. The measured north-south $|\Delta B|$ ratio is, however, consistent with the HLS current. Pertinent parameters from both satellite and surface data are tabulated in Table 2 for the passes of Figures 14-15 and for a pass which we shall discuss subsequently. An asterisk beside a surface field magnitude indicates that the observation was taken at a location favorable for comparison with the characteristics of HLS models given in the previous paragraph. By "favorable for comparison" is meant: (a) for ΔZ comparison the station should be in the vicinity of the vortex of the assumed HLS current, and (b) for ΔH comparison the station should be to the south of the vortex of the assumed HLS current, approximately under the eastward portion of the current. For example, on Sept. 2 the peak ΔB is -88γ, the surface ΔH is between 32γ and 60γ at the three observatories faborably located for ΔH comparison, and the surface ΔZ is -175γ at RB, which is in a location faborable for ΔZ comparison. These magnitudes, and those of the other passes in the table, are all consistent with the HLS models. Note than an electrojet causing positive bays of the magnitude shown in Table 2 could not possibly produce the magnitude of ΔB measured at the satellite.

Although the data discussed is in general agreement with the HLS models, the diversity of the negative ΔB for these passes indicates a large variability in strength and flow pattern of the source currents.

Another example, at a somewhat earlier MLT, is given in Figure 16 in which the negative ΔB region is smaller in extent. In the examples of Figures 14-15 BL is located to the south of the negative ΔB peak, whereas in Figure 16 BL is located to the north of the peak. Langel (1973a) noted that the surface data indicate a shift of the polar cap-auroral belt boundary near noon to the south during Toward sectors as compared to Away sectors. A shift southward is also expected at higher disturbance levels since under these conditions the auroral oval is known to expand southward (Feldstein, 1969). Both of these differences occur between the data of Figures 14-15 and Figure 16. In agreement with this shift and with the HLS current models, BL now shows a negative ΔH, indicating a polar-cap-like distribution rather than a positive bay. Other satellite-surface comparisons (see, for example, Table 2) are also in reasonable agreement with the HLS current models considering that the MLT of this pass is somewhat earlier than the MLT where the peak negative ΔB is expected; in particular, the N-S $|\Delta B|$ has the same characteristics as the data in Figures 14-15.

Correlation of Negative and Positive ΔB Region Disturbance

Although disturbance is usually present in both the positive and negative ΔB regions at the same time, there is not a one-to-one correlation in magnitude. Also, disturbance of one type sometimes occurs in the absence of the other type.

Comparison of Figures 14-16 illustrates this point. Positive ΔB is negligible in the data of Figure 15, small in the data of Figure 14, and moderate in Figure 16, whereas negative ΔB is significant in the data on all of these figures.

In none of these figures is $|\Delta B|$ to the south of the nightside auroral belt significant, although negative bay activity is present in the surface data from Figures 14 and 16. Thus the previous arguments against the westward electrojet as the source of the disturbance apply to this data also. It is noted that the positive peak in the data of Figure 16 probably contains a contribution from the westward electrojet.

Comparison of Satellite ΔB with Surface ΔZ in the Positive ΔB Region

To the north of the auroral belt, comparison of surface ΔZ with satellite ΔB when the satellite is directly over the observatory shows a high degree of correlation if negative bay activity is small or is far to the south of the observatory. Table 3 tabulates examples from Figures 14-16. For observatories near the satellite path which are relatively unaffected by the electrojet, ΔZ is usually almost equal to ΔB (within experimental error). This confirms that the non-electrojet source(s) causes a ΔB which is relatively constant with altitude.

Relation of Satellite ΔB and the AE Index

The extent to which electrojet currents are a source of ΔB at the POGO has already been noted. Examination of data from individual passes reveals further details regarding the relationships between the occurrence of disturbance at the

POGO in the positive and negative ΔB regions and the occurrence of electrojet activity. Briefly:

(1) When AE is high or moderate, the negative ΔB is always present at sunlit MLT, as in Figure 16.

(2) Disturbance is often present in the negative ΔB region when AE is low and sometimes when AE has been low for some hours (Figures 14-15).

(3) Quiet passes exist where the negative (and positive) ΔB is small.

Thus, while the level of disturbance in the negative ΔB region tends to be greater on days which are magnetically disturbed than on days which are relatively quiet, the negative ΔB region is not well correlated with electrojet activity.

Positive ΔB is usually:

(1) enhanced during periods of high electrojet activity,

(2) present for some hours after substantial electrojet activity has occurred and died away (Figures 14 and 16), and

(3) small when very little electrojet activity is evident for some hours prior to (and during) the data (Figure 15).

The second conclusion stated above is further illustrated in Figure 17. Three passes are shown during which AE is $\geqslant 500\gamma$, $< 100\gamma$ and $< 200\gamma$, respectively. (The Soviet observatories, not used to compute this AE, would not substantially modify AE during this period.) The positive ΔB during these passes reaches 150γ, 80γ, and 70γ, respectively. Significantly, for the second and third passes the positive ΔB region does not extend as far to the south in the midnight sector, and the ΔB distribution is close to a constant level throughout each pass. These facts indicate that the electrojet system has become small while the positive ΔB is only moderately reduced in magnitude.

Although much of the positive ΔB cannot be due to the electrojet, the magnitude of positive ΔB is correlated with electrojet activity to a greater extent than the magnitude of negative ΔB. The correlation coefficient between AL and the peak disturbance of individual passes through the positive ΔB region at altitudes <550 km. is 0.79.

THE EQUATORIAL CURRENT SHEET AS A SOURCE OF POSITIVE ΔB

A prominent feature of low latitude magnetic variation is a world-wide depression in H, particularly during some phases of magnetic storms. It is customary to resolve this variation into symmetric (Dst) and asymmetric (DS) components with respect to the earth's dipole axis. These definitions are not restricted to times during magnetic storms. Dst has been computed by Sugiura and Poros (1971) for the period 1957 to 1970. It has long been thought that during magnetic storms the Dst variations are caused by an equatorial ring current. More recent studies (e.g. Cain et al., 1962; Cahill, 1966; Cummings, 1966; Frank, 1967; Langel and Cain, 1968; Langel and Sweeney, 1971; Crooker and Siscoe, 1971) have shown that both Dst and low latitude DS are mainly due to sources external to the ionosphere, which implies an asymmetry in the ring current. Sugiura (1972a, b) has identified the ring current as an equatorial current sheet (ECS) which is a direct extension of the current sheet in the magnetotail.

A zero Dst does not imply that there is no ECS, as there is some arbitrariness in the assignment of a zero level for Dst (Sugiura, private communication). Sugiura (1973) has recently shown that at zero Dst the average ΔB at 2-3 Re is -45γ due to the quiet time ECS.

Because an ECS will result in positive ΔB at high latitudes, it must be considered as a source for the positive ΔB region. The relation between high latitude positive ΔB and the ECS is now briefly explored. It is clear from the references already cited, and from (unpublished) low latitude POGO data, that some asymmetry in the ECS exists even at low Kp. Apparently, however, a model does not exist which adequately represents the high latitude, low altitude, fields from an ECS which causes such a nonsymmetric equatorial disturbance.

Previous analyses (Chapman and Price, 1930; Rikitake and Sato, 1957; Langel and Sweeney, 1971) have noted that a time varying ring current will be accompanied by an induced current within the earth. A potential function of the form

$$V = \left[a\left(\frac{r}{a}\right)e + \left(\frac{a}{r}\right)^2 i\right]\cos\theta, \tag{1}$$

where a is the radius of the earth and θ is the (dipole) colatitude, was found to represent low and middle latitude data satisfactorily along a meridian. The terms in "e" and "i" are the external (ECS) and internal (induced) potentials, and the ratio R = i/e indicates the relative strength of the induced current. In the studies cited, all of which utilized data during magnetic storms, R was found to lie between 0.37 and 0.39.

To use (1) to estimate ΔB at high latitudes (e.g., approaching $\theta = 0$) for a particular ΔB at the equator ($\theta = \pi/2$), the average equatorial ΔB from POGO for Kp $\geqslant 4^-$, 2^- to 3^+, and 1^- to 1^+ has been computed. In all cases the equatorial ΔB is asymmetric; the average equatorial ΔB is about -5 to -55γ, 0 to -25γ, and 0 to -15γ for Kp $\geqslant 4^-$, 2^- to 3^+, and 1^- to 1^+, respectively. Using (1) with R = 0.38, and taking the equatorial ΔB to be -55γ, -25γ, and -15γ, respectively, gives a high latitude positive ΔB of 9.6γ, 4.4γ, and 2.6γ. These positive ΔB values are negligible in comparison to the average non-electrojet positive ΔB. If, however, R is between 0 and 0.1, the high latitude ΔB, from (1), becomes 40-50γ, 18-25γ, and 11-15γ, respectively, which is sufficient to account for most of the average non-electrojet positive ΔB. Although these results indicate that the ECS could be the major source, the result is inconclusive because R is not accurately known and the equatorial ΔB asymmetry is not taken into account in the computation.

To investigate the statistical correlation between the positive ΔB region and the ECS, it is assumed that Dst reflects the strength of the ECS. As a measure of the positive ΔB, the quantity BP is defined as the peak value of positive ΔB on each satellite pass. Only those passes whose local times are near the peak value of the average positive ΔB are considered, and the satellite data is limited to altitudes above 700km to minimize the electrojet contribution to BP. Because a correlation with the westward electrojet strength, as measured by the AL index, is included in the analysis, the universal times of the satellite passes are restricted so that at least one of the observatories used to compute AL is in the $1\text{-}5^h$ MLT region. Figure 18 is a scatter plot of BP vs Dst. A linear least squares fit to this data gives the equation

$$BP = 23.7 - 1.28\,Dst\ (\gamma), \tag{2}$$

with a standard deviation of 25γ. If a term for AL is included in the least squares fit, the result is

$$BP = 15.6 - 0.97\,Dst - 0.139\,AL\ (\gamma), \tag{3}$$

with a standard deviation of 19.6γ. The correlation coefficient between BP and Dst is -0.63.

Although BP tends to increase with decreasing Dst, a correlation coefficient of -0.63 is not high, and, moreover, a significant number of points are in large disagreement with equations (2) and (3). These results must be regarded as inconclusive. While it is possible that the ECS contributes substantial positive ΔB at high latitudes, it is also possible that the observed degree of correlation results from a tendency for all sources of near-earth magnetic disturbance to increase in intensity at approximately the same time.

Magnetopause currents will have some effect both on Dst and on the ΔB measured by the POGO. From model computations (see e.g. Mead, 1964) we know that the equatorial field, in the vicinity of the earth's surface, from magnetopause currents is of the order of 25γ with peak to peak daily variations of the order of 8γ. Variation of the magnetopause boundary from 12 to 9 Re could cause an increase in the equatorial field at the surface of about 25γ. This is the range expected except during large sudden commencements. Variations in ΔB

at high latitudes due to magnetopause currents are smaller than those at the equator, for example, the model of Sugiura and Poros (1973) gives a positive ΔB, at high latitudes, near the earth of 10-15γ due to both magnetopause currents and the ECS. It is concluded that magnetopause currents are not likely to contribute substantially to the high latitude ΔB and contribute at most a 10-20γ variation to Dst, except during large magnetopause compressions.

If the ECS contributes to the polar positive ΔB, it is unlikely that such a contribution is restricted in MLT as is the measured positive ΔB region. The implication is that a positive ΔB due to the ECS may be present over the entire polar cap, and that the source of the negative ΔB region is strong enough to overwhelm this positive ΔB. If this is true, and the resulting positive ΔB is not uniform in MLT, then the MLT distribution of positive and negative ΔB may be somewhat different than shown in Figure 1. Comparison of summer and winter average ΔB contour plots indicates that the shape of the negative ΔB region does not change drastically from winter to summer, although the amplitude varies by about a factor of 3 at altitudes $\leqslant$550 km. This, together with the agreement between the average measured surface disturbance and that computed from the HLS currents, indicates that the measured MLT distribution of negative ΔB is close to the actual MLT distribution of negative ΔB caused by ionospheric currents (HLS).

Need for a Source of Positive ΔB other than the Equatorial Current Sheet and the Electrojet

Examination of individual satellite passes indicates that, in many cases, an estimated contribution of $\Delta B = 20 - \mathrm{Dst}$ (γ) from the ECS, together with a reasonable estimate of disturbance from the westward electrojet, is close to the measured positive ΔB. However, it is also possible to find examples where the measured positive ΔB is considerably different from these estimates.

Figure 19 illustrates several cases where the measured positive ΔB differs considerably from the estimated positive ΔB. Consider first parts (a) and (b) of the figure for which Dst is -7γ and $+4\gamma$, respectively. With regard to the electrojets, AL is -20γ and -70γ, respectively, and ΔH is indicated on the plots for selected non-AE observatories (AE observatories are underlined). For (a) the maximum negative ΔH is -115γ at BW near 7.5^h MLT, well away from the POGO track; observatories in the auroral belt at 0-4^h MLT show very little disturbance. For (b) auroral belt disturbance is again small from 0-5^h MLT, but there is some negative bay activity from 6^h to 12^h MLT, namely $\Delta H = -250\gamma$, -104γ, and -340γ at FC, BL, and GO, respectively. Of these, FC and (particularly) GO are at some distance from the satellite track. At most, the contribution to POGO ΔB for these altitudes should be 1/10 the maximum ΔH due to an electrojet, which gives about 12γ for (a) and 35γ for (b). We believe these estimates are high because the observatories at which maximum $|\Delta H|$ occurs are not close to the satellite path, and the surface disturbance is more localized than that represented by the numerical electrojet models. A localized jet-current will result in less ΔB at POGO than predicted by the models. Contributions from the ECS for Dst = -7γ and 4γ should be no more than 33γ and 20γ, respectively, so that the <u>maximum</u> BP expected from electrojet and ECS is 45γ and 55γ for (a) and (b), respectively, while the measured BP are 60γ and 72γ.

Plots (c) and (d) of the figure show data where BP is $\leqslant 30\gamma$ and $\leqslant 45\gamma$, respectively (in fact, ΔB is less than 20γ and 35γ, respectively, over most of these passes), yet Dst is -29γ and 64γ, respectively, so that much higher positive ΔB (about 49γ and 84γ, or more, depending on the electrojet contribution) would be expected if the ECS and westward electrojet were the sources of the positive ΔB.

SUMMARY AND CONCLUSIONS

This study has used magnetic field measurements from the POGO spacecraft and from observatories to test prevalent concepts regarding the current systems causing high latitude magnetic disturbance and to extend understanding of the morphology of the measured disturbance and its sources. Excluding variations between interplanetary magnetic sectors, Figure 20 summarizes the proposed source current distribution, and Table 4 indicates, in a broad sense, which sources are believed to be important contributors to disturbance at various altitudes.

The existence and characteristics of the eastward and westward electrojets will be discussed more fully in a subsequent paper. In this study: (a) It is demonstrated that <u>much</u> of the <u>positive ΔB</u> at the POGO, and positive ΔZ at the surface, from 22^h to 10^h MLT, is not due to an ionospheric source either of the jet-type or of the DP2 type. The average electrojet contribution to positive ΔB, as determined from numerical models, is about 25γ and 10γ at 460km and 800km, respectively, for $Kp = 2^-$ to 3^+. However, the measured maximum contour of the average positive ΔB (again for Kp = 2^- to 3^+) is about 52γ and 44γ at 460km and 800km, respectively; the non-electrojet portion of the positive ΔB is roughly constant with altitude, and its peak magnitude is estimated to be about 50-80γ, 20-30γ, and 7-15γ for Kp $\geqslant 4^-$, 2^- to 3^+, and 1^- to 1^+, respectively. A portion of this positive ΔB is likely due to the ECS, but some of the data are not accounted for by estimates of ΔB from this source. Rough estimates of the percentage of ΔB from electrojet and non-electrojet (mainly extra-ionospheric) sources are given in Table 4. Surface ΔZ must also contain a component from the "constant" ΔB (assuming $\Delta B \approx \Delta Z$), and indeed, if an estimate of this "constant" ΔZ component is subtracted from the measured average surface ΔZ, the remaining ΔZ is more consistent with an electrojet source than is the measured ΔZ. (b) A need for an ionospheric current of broad dimensions, <u>the HLS current</u>, is established at sunlit local times. In this region, roughly from 12^h to 22^h MLT (the local time, near 19^h, to which the HLS current extends is dependent on season), the magnetic field at the satellite is characteristically weakened ($\Delta B < 0$) above invariant latitudes of about 65°. That the negative ΔB region is essentially a "daylight" phenomenon is indicated by its seasonal variation (greatest magnitude in summer, least in winter) and by the location of the peak of the average ΔB at about 15^h MLT. A similar seasonal variation is also present in the average surface data (Langel, 1973a). Average ΔB in this region decreases rapidly with altitude; in fact, during winter the average negative ΔB above 900km. is negligible. Previous studies have suggested that the currents causing some of the positive bay disturbance are of broad latitudinal dimensions and flow in the sunlit E-region of the ionosphere where their intensity is determined by solar radiation controlled conductivity. Our measurement of the altitude variation of ΔB in this region is strong evidence that the satellite negative ΔB is caused by ionospheric currents below satellite altitudes (400km). The fact that the negative ΔB region is negligible above 900km in winter suggests strongly that all of the negative ΔB in this region is due to ionospheric sources.

Not only is the HLS current able to cause the major features of the satellite negative ΔB region, but it is also able to cause the major features of the surface positive bay variations from 13^h to 19^h MLT and some of the features of the surface polar cap magnetic variation. Such current systems are, of course, averages and do not represent localized phenomena often detected at observatories.

Modifications to such current systems will also be necessary to account for spatial gradients in conductivity and electric field, and to account for the presence of field aligned currents. With such qualifications in mind, however, major features of the derived current systems are probably representative of real current flow. In particular, the general direction and approximate magnitude of the model currents where the conductivity gradients are not large (perhaps for solar zenith angles less than about 75°; see, e.g., Keneshea et al., 1970) are expected to be close to the averages of the real current.

No attempt is made to show continuity in Figure 20 in some regions where we believe that field aligned currents are important. This is particularly true near dusk and dawn in the auroral belt and over the dark portion of the polar cap. It is entirely possible that part or all of the HLS current flows into the eastward electrojet.

The dashed curves on the morning side of noon indicate current flow needed to account for the average horizontal disturbance at the earth's surface and for positive ΔB during Toward interplanetary magnetic field sectors. Some observatory data, such as that of Figure 19b, support the reality of this current but seem to indicate closure via magnetic field aligned currents rather than by currents flowing into the westward electrojet.

In a subsequent paper it will be shown that variations in the positive and negative ΔB regions do not correlate with DP2 fluctuations as defined by Nishida and his co-workers (e.g. Nishida and Kokubun, 1971, and references therein). However, the existence of a spatially broad ionospheric current in the positive ΔB region is not ruled out. The inferred altitude variation of the non-electrojet contribution to the positive ΔB is uncertain enough that some contribution could arise from a non-jet type source at sunlit local times. If such a source exists and is highly variable, it might account for the deviations of the positive ΔB from that which is expected from the ECS and the westward electrojet.

ACKNOWLEDGMENTS

This work is based on a thesis submitted in partial fulfillment of the requirements for the Ph.D. at the University of Maryland. I wish to thank my thesis advisor, Dr. T. J. Rosenberg, for guidance throughout the work. I would also like to thank Dr. D. A. Tidman of the University of Maryland and Dr. J. C. Cain, Dr. J. P. Heppner, and Dr. M. Sugiura of Goddard Space Flight Center for suggestions and critical discussion.

REFERENCES

Akasofu, S. -I., S. Chapman, and C. -I. Meng, The Polar Electrojet, Jour. of Atm. Terr. Phys., 27, 1275, 1965.

Bohse, J. R., and T. L. Aggson, Average ionospheric electric field distribution, presented at the Spring 1973 meeting of the AGU, EOS, Trans. AGU, 54, 417, 1973.

Cahill, L. J., Inflation of the inner magnetosphere during a magnetic storm, J. Geophys. Res., 71, 4505, 1966.

Cain, J. C., I. R. Shapiro, J. D. Stolarik, and J. P. Heppner, Vanguard 3 magnetic field observations, J. Geophys. Res., 67, 5055, 1962.

Chapman, S., and A. T. Price, The electric and magnetic state of the interior of the earth as inferred from terrestrial magnetic variations, Phil. Trans. Roy. Soc. London, A229, 427-460, 1930.

Crooker, N. U., and G. L. Siscoe, A study of the geomagnetic disturbance field asymmetry, Radio Sci., 495-501, 1971.

Cummings, W. D., Asymmetric ring currents and the low-latitude disturbance daily variation, J. Geophys. Res., 71, 4495, 1966.

Feldstein, Y. I., Polar auroras, polar substorms, and their relationships with the dynamics of the magnetosphere, Rev. Geophys., 7, 179-218, 1969.

Feldstein, Y. I., and A. N. Zaitzev, Magnetic field variations at high latitudes on quiet days in summer during the IGY, Geomag. i. Aeronomie, 7, 160, 1967.

Feldstein, Y. I., and A. N. Zaitzev, Quiet and disturbed solar daily variations of magnetic field at high latitudes during the IGY, Tellus, 20, 338, 1968.

Forbush, S. E., and M. Casaverde, Equatorial electrojet in Peru, Carnegie Inst. of Wash. Pub., 620, 1961.

Frank, L. A., On the extraterrestrial ring current during geomagnetic storms, J. Geophys. Res., 72, 3753-3761, 1967.

Fukushima, N., Gross character of geomagnetic disturbance during the International Geophysical Year and the Second Polar Year, Rep. Ionos. Space Res. Japan, 16, 37-56, 1962.

Heppner, J. P., A study of relationships between the aurora borealis and the geomagnetic disturbances caused by electric currents in the ionosphere, Thesis, Calif. Inst. of Techn., 1954 (also published as Defense Research Board, Canada, Rpt. No. DR135, 1958).

Heppner, J. P., J. D. Stolarik, and E. M. Wescott, Electric field measurements and the identification of currents causing magnetic disturbances in the polar cap, J. Geophys. Res., 76, 6028, 1971.

Kamide, Y. and N. Fukushima, Positive geomagnetic bays in evening high-latitudes and their possible connection with partial ring current, Rept. Ionos. Space Res. Japan, 26, 79, 1972.

Kawasaki, K., and S. -I. Akasofu, Polar solar daily geomagnetic variations on exceptionally quiet days, J. Geophys. Res., 72, 5363, 1967.

Keneshea, T. J., R. S. Narcisi, and W. Swider, Jr., Diurnal model of the E region, J. Geophys. Res., 75, 845, 1970.

Kokubun, S., Polar substorm and interplanetary magnetic field, Planet. Space Sci., 19, 697-714, 1971.

Langel, R., Average high latitude magnetic field: Variation with interplanetary sector and with season. I. Disturbed conditions, Planet. Space Sci., 21, 839-855, 1973a.

Langel, R. A., Near earth disturbance in total field at high latitudes, I. Summary of data from OGO's 2, 4, and 6, Submitted to J. Geophys. Res., 1973b.

Langel, R. A., and J. C. Cain, OGO-2 magnetic field observations during the magnetic storm of March 13-15, 1966, Ann. Geophys., 24, 857-869, 1968.

Langel, R. A., and R. E. Sweeney, Asymmetric ring current at twilight local time, J. Geophys. Res., 76, 4420-4427, 1971.

Mead, Gilbert D., Deformation of the geomagnetic field by the solar wind, J. Geophys. Res., 69, 1181, 1964.

Meng, C. -I., and S. -I. Akasofu, Polar magnetic substorms in the conjugate areas, Radio Sci., 3, 751, 1968.

Nagata, T., and S. Kokubun, An additional geomagnetic daily variation Field (S_q^p -field) in the polar region on geomagnetically quiet day, Rept. Ionos. Space Res. Japan, 16, 256, 1962.

Nishida, A., Geomagnetic DP2 fluctuations and associated magnetospheric phenomena, J. Geophys. Res., 73, 1795, 1968a.

Nishida, A., Coherence of geomagnetic DP2 fluctuations with interplanetary phenomena, J. Geophys. Res., 73, 5549, 1968b.

Nishida, A., DP2 and polar substorm, Planet. Space Sci., 19, 1971.

Nishida, A., N. Iwasaki, and T. Nagata, The origin of fluctuations in the equatorial electrojet; a new type of geomagnetic variation, Ann. Geophys., 22, 478, 1966.

Nishida, A., and K. Maezawa, Two basic modes of interaction between the solar wind and the magnetosphere, J. Geophys. Res., 76, 2254, 1971.

Nishida, A., and S. Kokubun, New Polar magnetic disturbances, S_q^p, SP, DPC, and DP2, Rev. Geophys. Space Phys., 9, 417, 1971.

Rikitake, T. and S. Sato, The geomagnetic Dst field of the magnetic storm on June 18-19, 1936, Bull. Earthquake Res. Inst., Tokyo Univ., 35, 7-21, 1957.

Scrase, F. J., The electric current associated with polar magnetic substorms, J. Atm. Terr. Phys., 29, 567, 1967.

Stagg, J. M., The diurnal variation of magnetic disturbance in high latitudes, Proc. Roy. Soc. London, A149, 298-311, 1935.

Sugiura, M., The ring current, in Critical Problems of Magnetospheric Physics, Proceedings of the joint COSPAR/IAGA/URSI symposium, Madrid, Spain, 11-13 May 1972, ed. by E. R. Dyer, IUCSTP secretariat c/o National Academy of Sciences, Washington, D.C., 1972a.

Sugiura, M., Equatorial current sheet in the magnetosphere, J. Geophys. Res., 77, 6093, 1972b.

Sugiura, M., Quiet-time magnetospheric field depression at 2.3 to 3.6Re, J. Geophys. Res., 78, 3182, 1973.

Sugiura, M., and D. J. Poros, Hourly values of equatorial Dst for the years 1957 to 1970, NASA/GSFC Report X-645-71-278, Goddard Space Flight Center, Greenbelt, Md., July 1971.

Sugiura, M., and J. P. Heppner, Electric and magnetic fields in the earth's environment, American Institute of Physics Handbook, 3rd ed., McGraw Hill, 1972.

Table 1

Observatories Used in Analysis

Station	Mnemonic	Geomagnetic Position		Geographic Position	
		Latitude	Longitude	Latitude	Longitude
Alert	AT	85.8	188.1	82°30'	-62°30'
Baker Lake	BL	73.7	315.2	64°20'	-96°2'
Barrow	BW	68.5	241.1	71°18'	-156°45'
Cape Chelyuskin	CC	66.2	176.4	77°43'	104°17'
College	CO	64.6	256.5	64°52'	-147°50'
Dikson Is.	DI	63.0	161.5	73°33'	80°34'
Dombas	DO	62.2	100.1	62°4'	9°7'
Heiss Is. (Druzhnaya)	DR	71.3	156.0	80°37'	58°3'
Fort Churchill	FC	68.7	322.8	58°48'	-94°6'
Godhavn	GO	79.8	32.5	69°14'	-53°31'
Great Whale River	GWR	66.5	347.4	55°16'	-77°47'
Lovo	LO	58.0	105.7	59°21'	17°50'
Leirvogur	LR	70.2	71.0	64°11'	21°42'
Meanook	ME	61.8	301.1	54°30'	-113°20'
Mould Bay	MLB	79.0	256.3	76°12'	-119°24'
Newport	NT	55.0	300.1	48°16'	-117°7'
Resolute Bay	RB	82.9	289.3	74°42'	-94°54'
Rude Skov	RS	55.8	98.5	55°51'	12°27'
Sitka	SI	59.9	275.4	57°4'	-135°20'
Sodankyla	SO	63.7	119.9	67°22'	26°38'
Thule	TH	88.9	358.0	77°29'	-69°10'
Tiksi	TI	60.4	191.4	71°35'	129°0'

Table 2

Comparison of Satellite and Ground Disturbance from the Negative ΔB Region

Data is from Figures 14-16

Field Quantity	Date of Pass		
	9/2	9/5	9/19
Peak Satellite $-\Delta B$	-88γ	-53γ	-67γ
Surface ΔH: FC	32γ*	20γ*	52γ*
BL	60γ*	40γ*	-193γ
GWR	50γ*	60γ*	120γ*
ΔZ at RB	-175γ*	—	120γ
ΔZ at FC	10γ	-25γ	-50γ*
Kp during pass	1°	1^{-}	4°
Interplanetary Sector	Away	Away	Toward

*Observation taken at a location favorable for comparison with the HLS current models.

Table 3

Comparison of Surface ΔZ with Satellite ΔB

Figure	Station	Surface ΔZ (γ)	Satellite ΔB (γ)
14	DR	5	10
15	DI	0	0
15	CC	10	10-20
15	AT	10	8
16	AT	35	32
16	TH	40	35

Table 4

Probable Sources for Disturbance at Various Altitudes

MLT Range	Disturbance Characteristics	Altitude				
		Surface	400 km	600 km	800 km	1000 km
23^h to $8-10^h$	Negative Bay (Surface ΔH)	W E J	—	—	—	—
	Positive ΔB	W E J (70%) X-tra I. (30%)	W E J (50%) X-tra I. (50%)	W E J (34%) X-tra I. (66%)	W E J (22%) X-tra I. (78%)	W E J (10%) X-tra I. (90%)
13^h to $18-20^h$ (sunlit)	Positive Bay (Surface ΔH)	HLS	—	—	—	—
	Negative ΔB	HLS	HLS	HLS	HLS	HLS
$18-20^h$ to 23^h (dark)	Positive Bay (Surface ΔH)	E E J (HLS)	—	—	—	—
	Negative ΔB	E E J (HLS)	E E J (HLS)	E E J (HLS)	Very Small Disturbance	
$8-10^h$ to 13^h	Confused Region, can have positive or negative bays and positive or negative ΔB. Our study indicates the existence of a broad current in this region during Toward interplanetary sectors but is inconclusive otherwise.					

Abbreviations for sources: W E J = westward electrojet (ionospheric); E E J = eastward electrojet (ionospheric); HLS = HLS-like current (ionospheric); X-tra I. = non-ionospheric sources (ECS, Magnetopause Currents, etc.); ( ) denotes possible source, our results inconclusive.

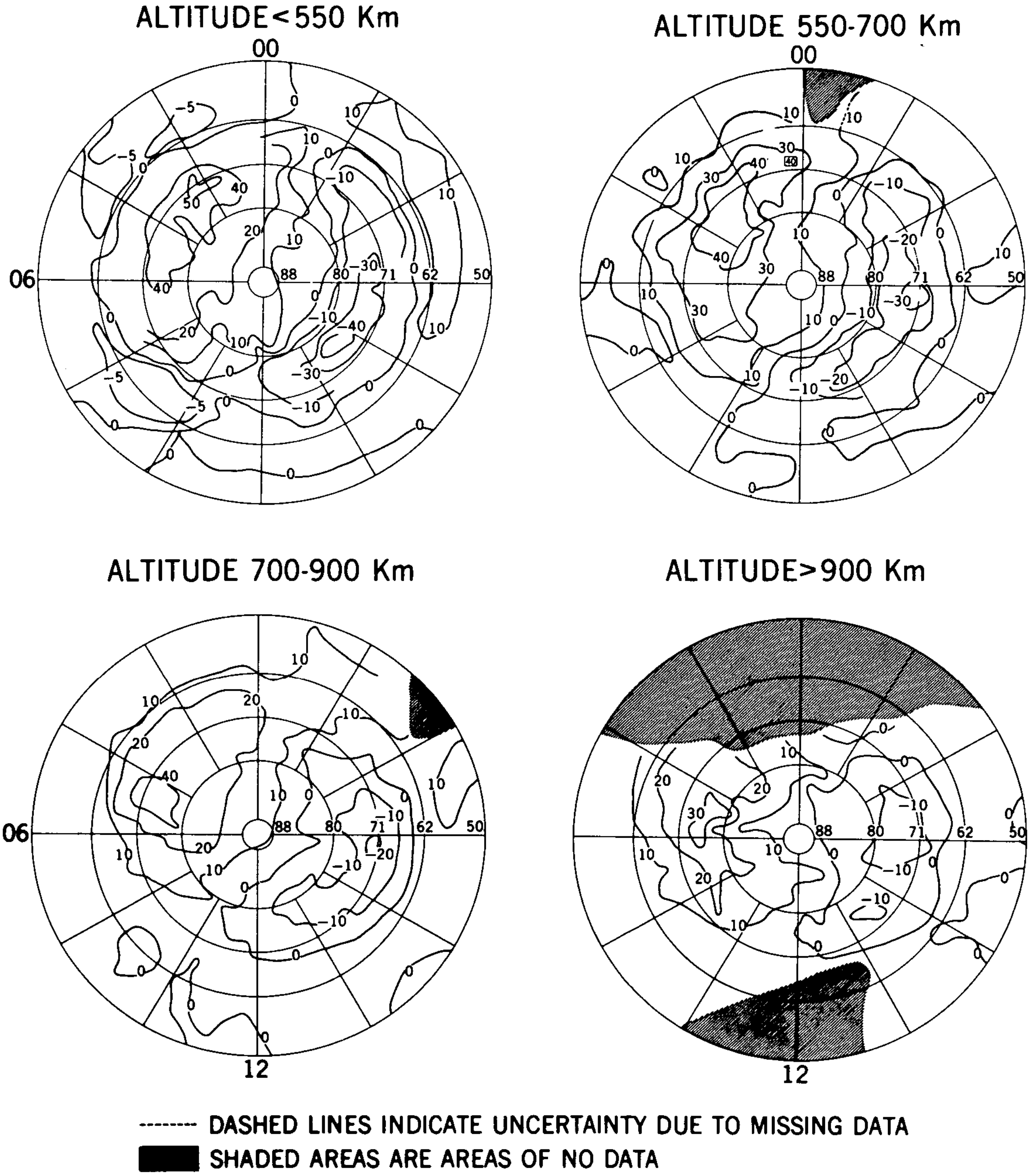

Figure 1. Average ΔB from OGO 2, 4, and 6, northern hemisphere, $Kp = 2^-$ to 3^+, months 3, 4, 9, and 10. Coordinates are MLT and dipole latitude.

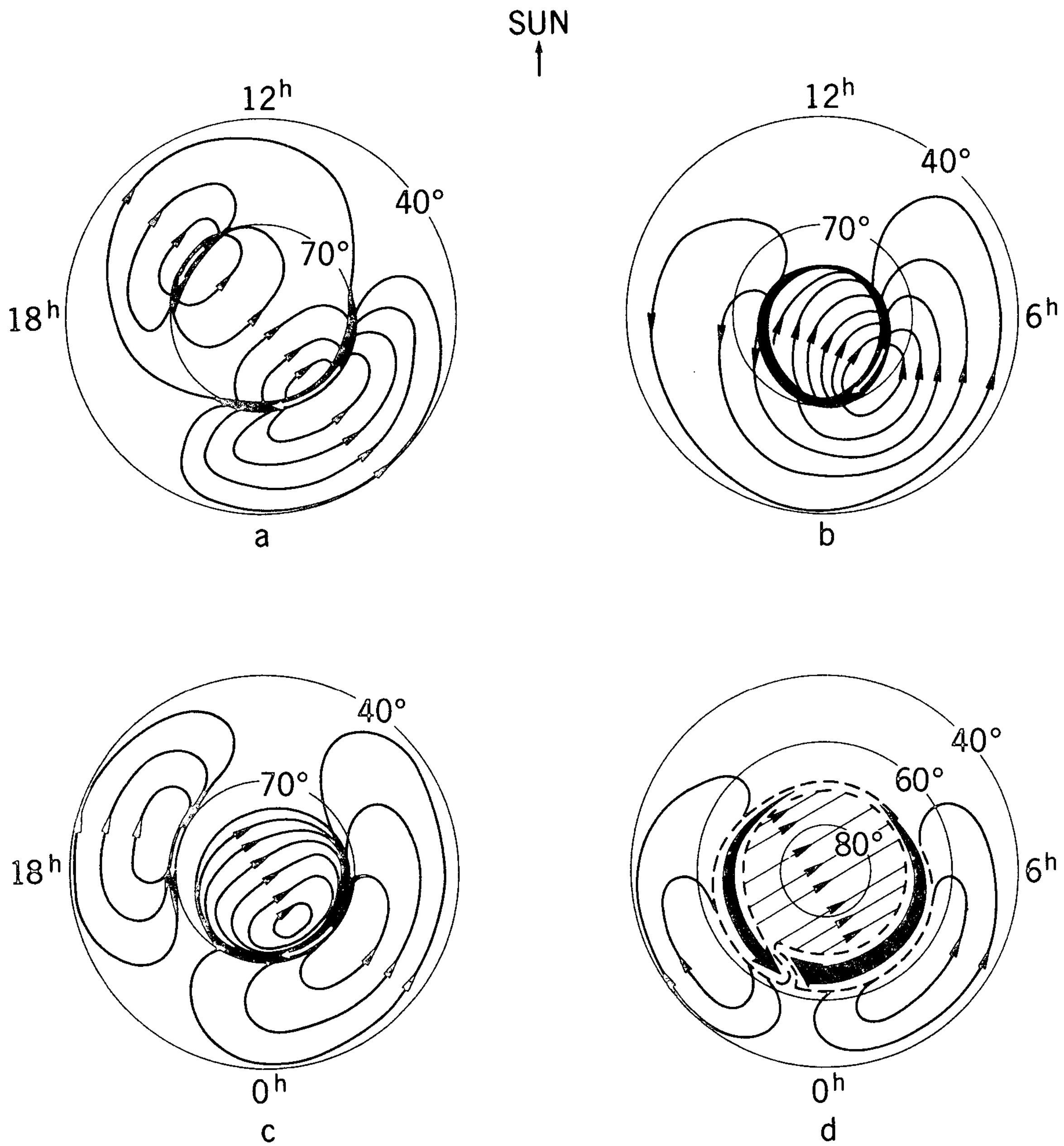

Figure 2. Equivalent current systems for the auroral electrojet. (a) is the classical two-celled (DS) system, (b) is from Akasofu et al. (1965), (c) is from Feldstein (1969), and (d) is from Sugiura and Heppner (1972).

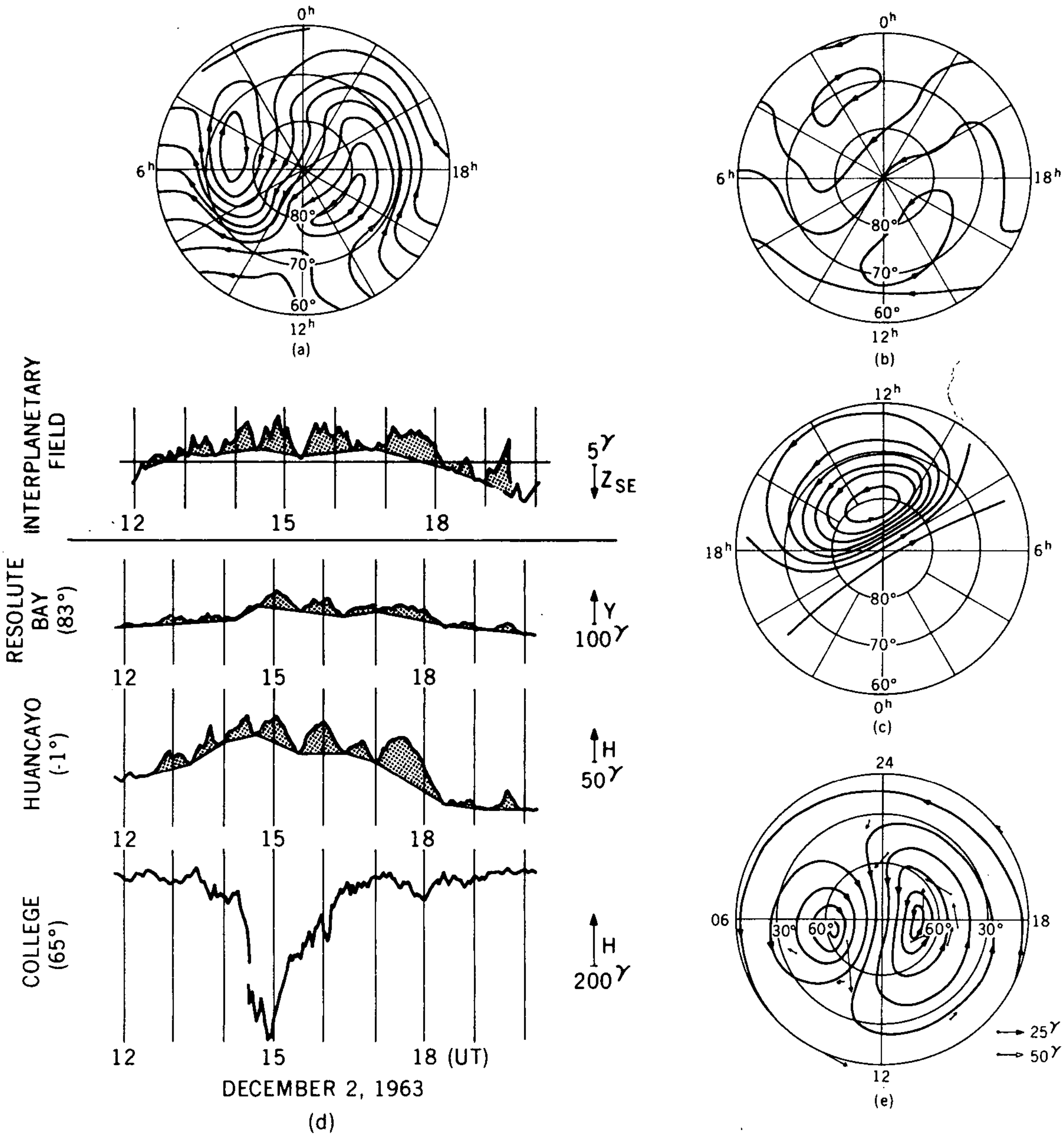

Figure 3. Non-electrojet current systems. (a) and (b) are the northern hemisphere equivalent current systems of mean daily variations on quiet days from Nagata and Kokubun (1962). (a) is for the June solstice and (b) is for the December solstice. 2×10^4 amps flows between stream lines. (c) is the DPC current from Feldstein (1969), 10^4 amps flows between stream lines. (d) and (e) are DP2 for Dec. 2, 1963, from Nishida and Kokubun (1971). In (d) records of DP2 are shaded. (e) is the equivalent current system of DP2 with 5×10^4 amp between stream lines.

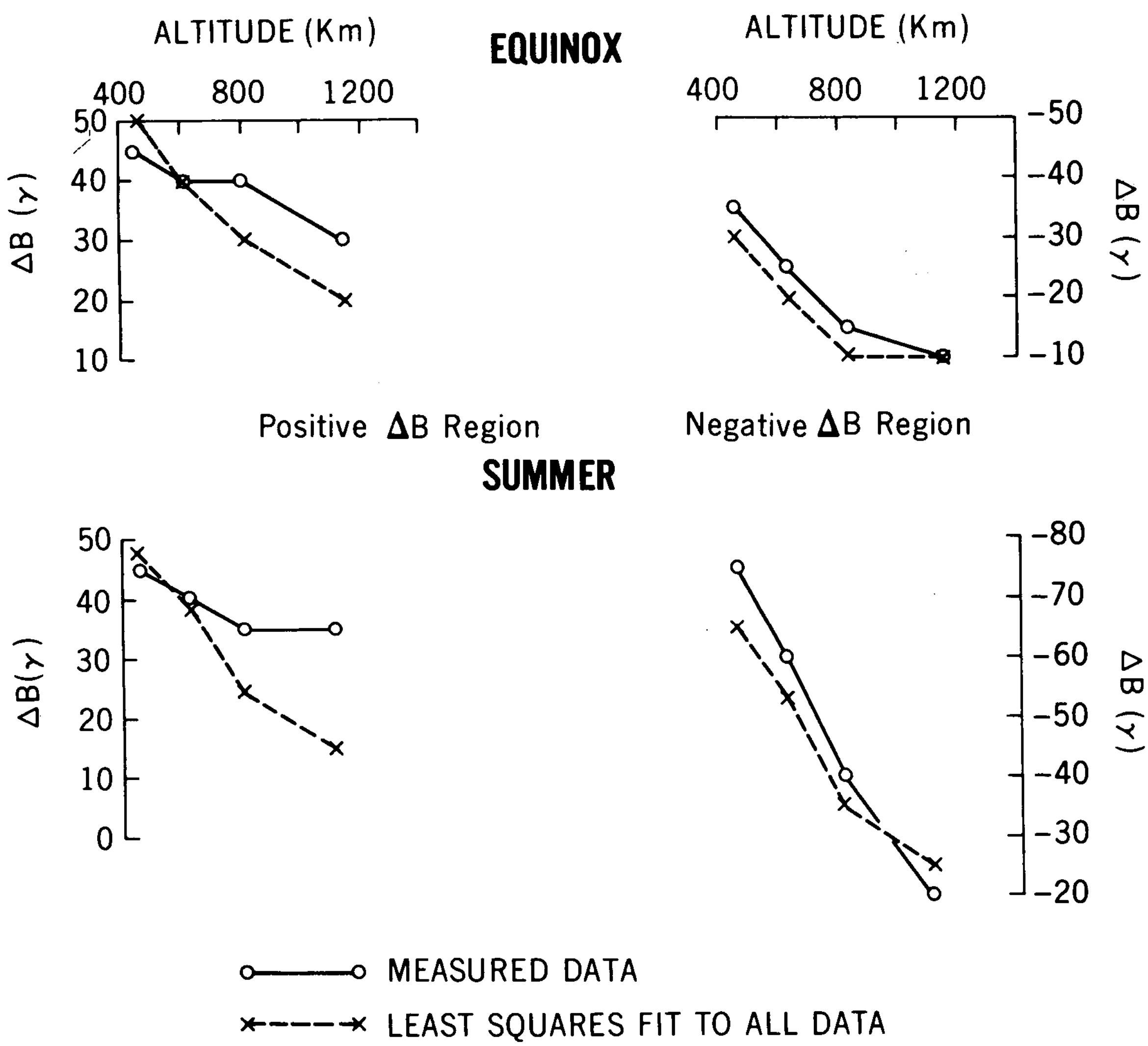

Figure 4. Altitude variation of ΔB from the measured data and from the best-fit equivalent current system. Northern hemisphere.

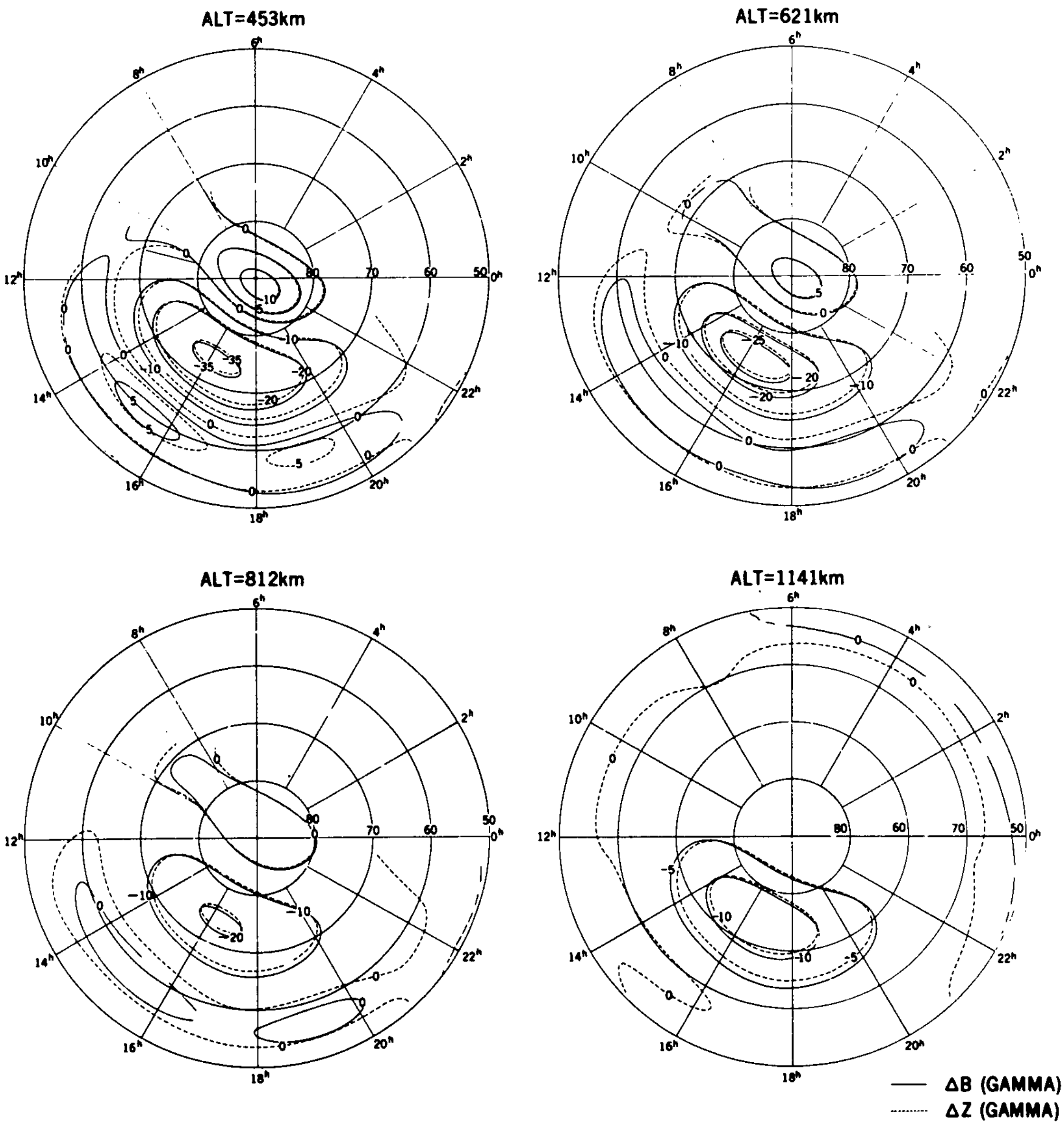

Figure 5. Disturbance (ΔB and ΔZ) computed from potential function derived from data in the negative ΔB region. Northern hemisphere, Kp = 2^- to 3^+, months 3, 4, 9, and 10. Coordinates are MLT and dipole latitude.

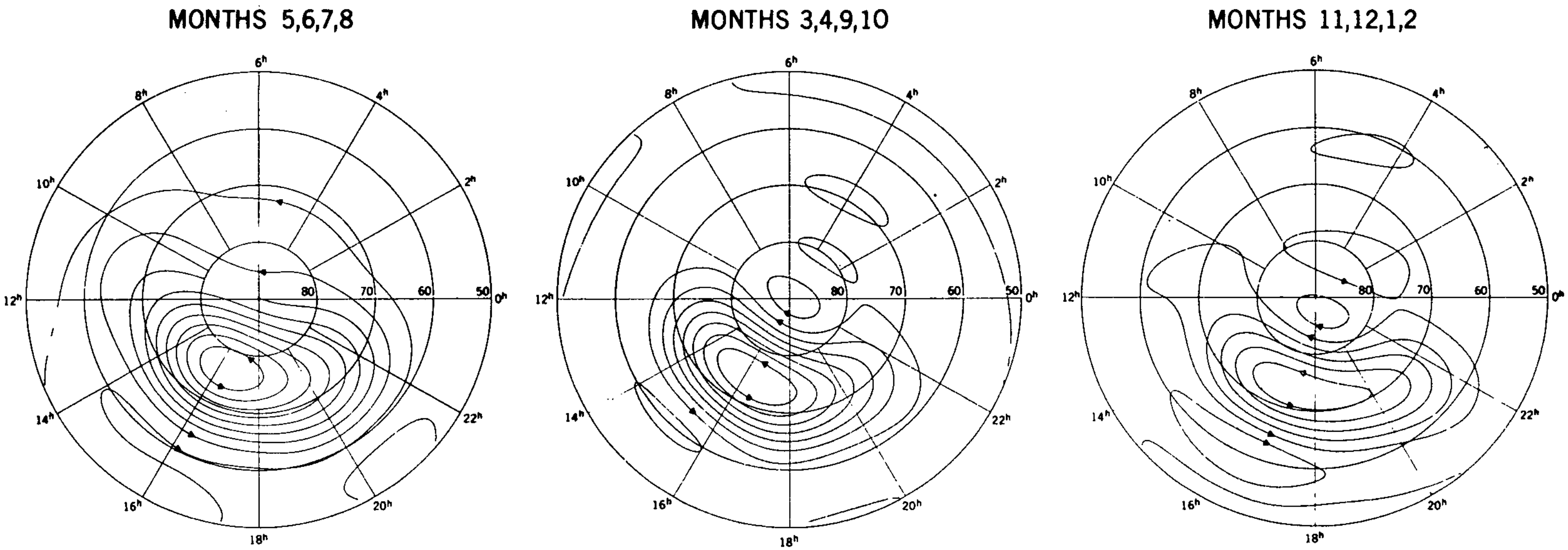

Figure 6. HLS currents derived from data in the negative ΔB region for Kp = 2^- to 3^+. Current is assumed to flow at 115 km, 10^4 amps flows between stream lines. Coordinates are MLT and dipole latitude.

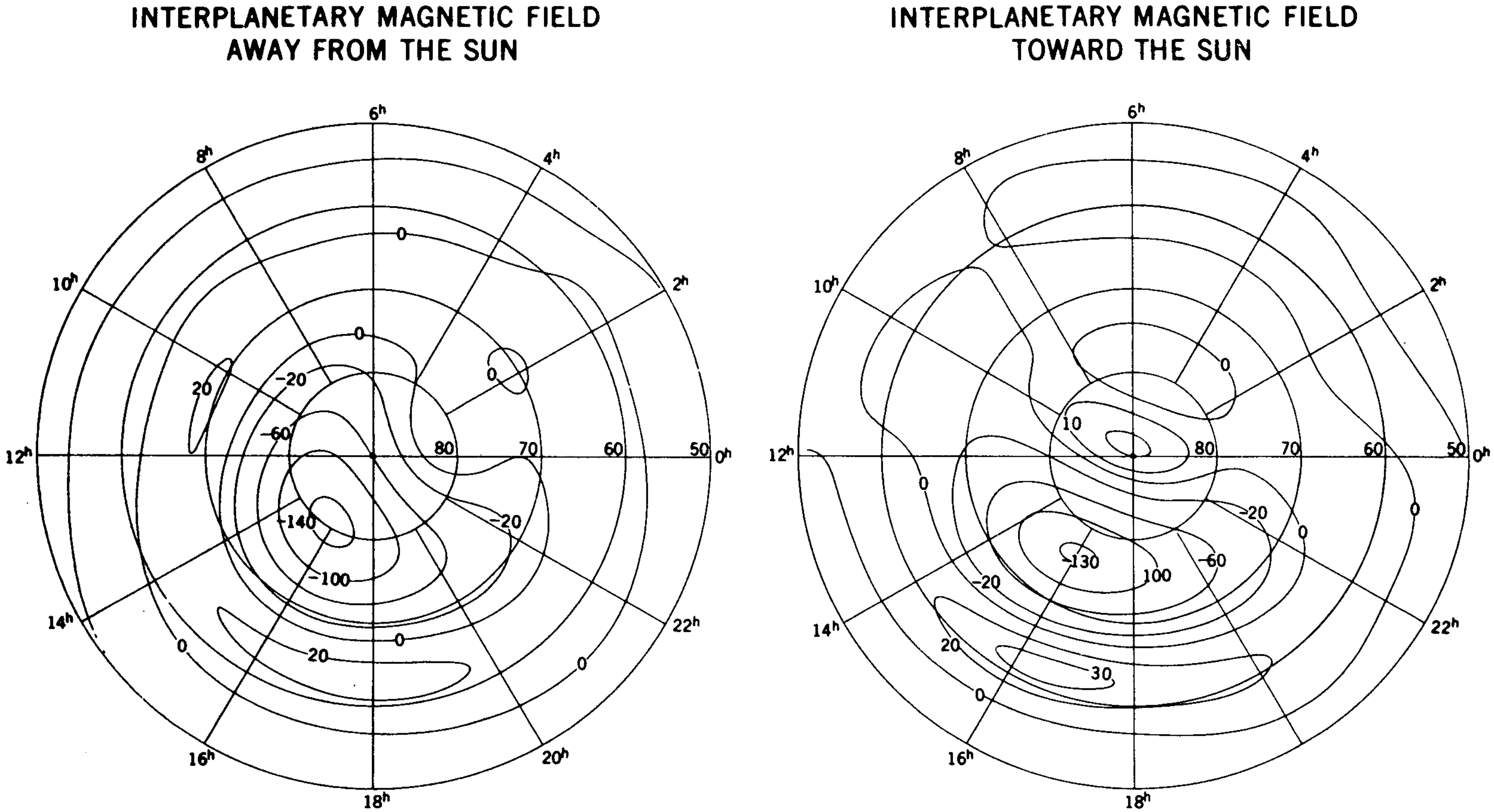

Figure 7. ΔZ (γ) at the earth's surface from the HLS current system for geomagnetic summer and Kp = 2^- to 3^+. Coordinates are MLT and invariant latitude.

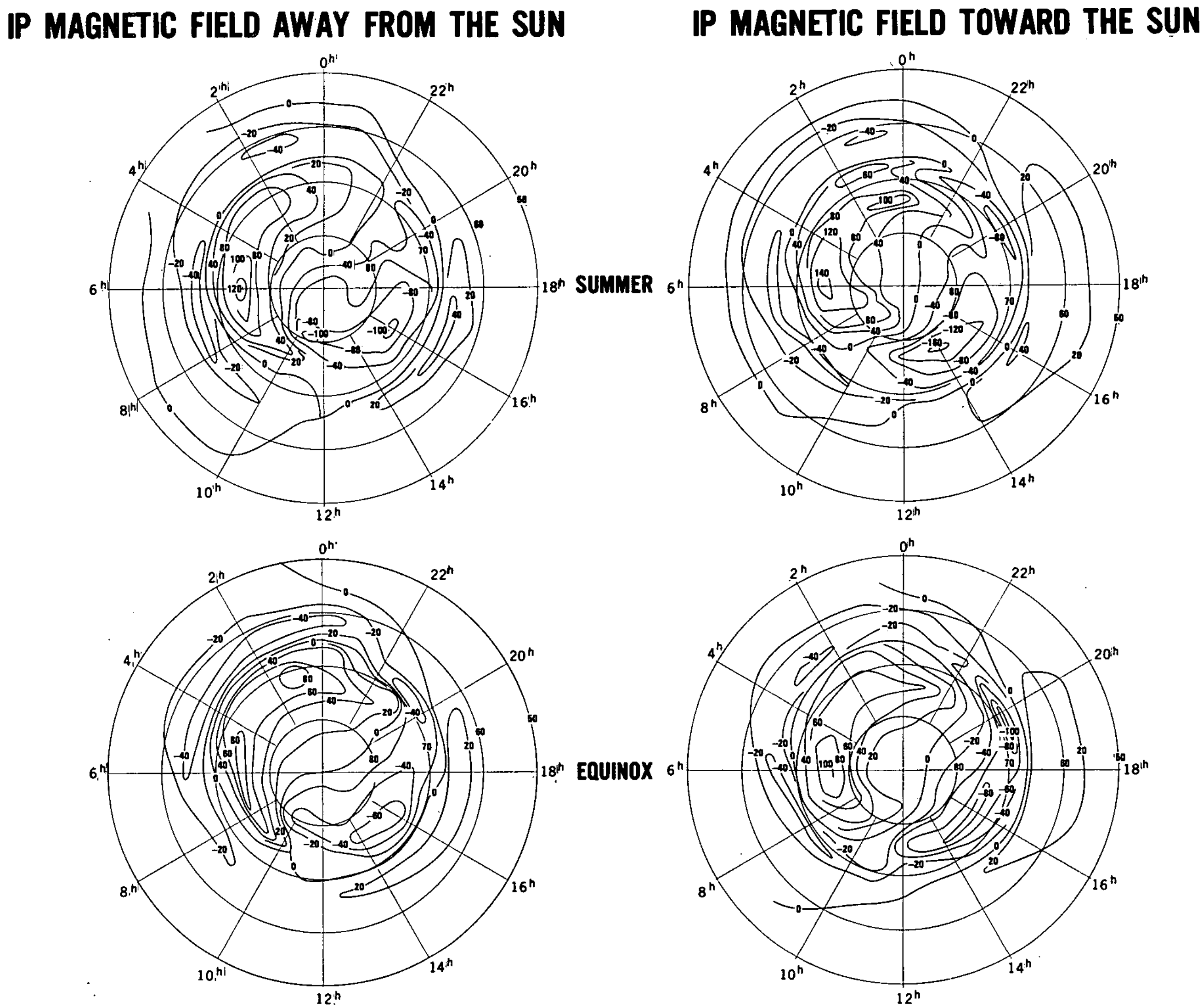

Figure 8. Average ΔZ (γ) at the earth's surface (Langel, 1973a). Geomagnetic seasons, $Kp = 2^{-}$ to 3^{+}. Coordinates are MLT and invariant latitude.

MEASURED AVERAGE HORIZONTAL DISTURBANCE AT THE EARTH'S SURFACE

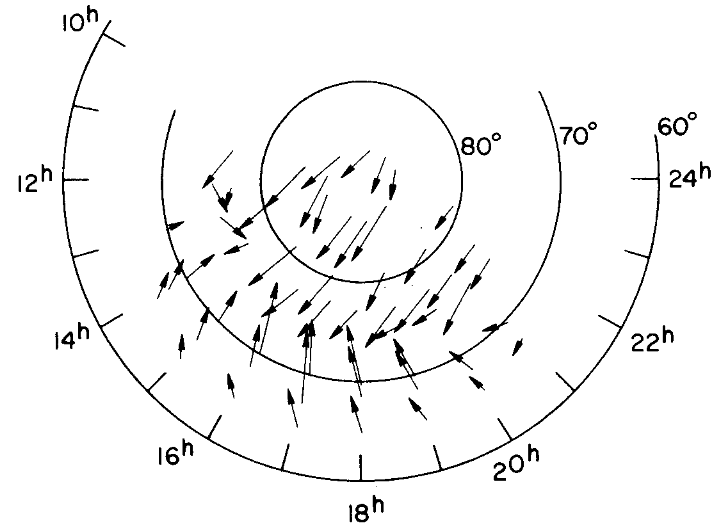

HORIZONTAL DISTURBANCE AT THE EARTH'S SURFACE FROM THE HLS CURRENT

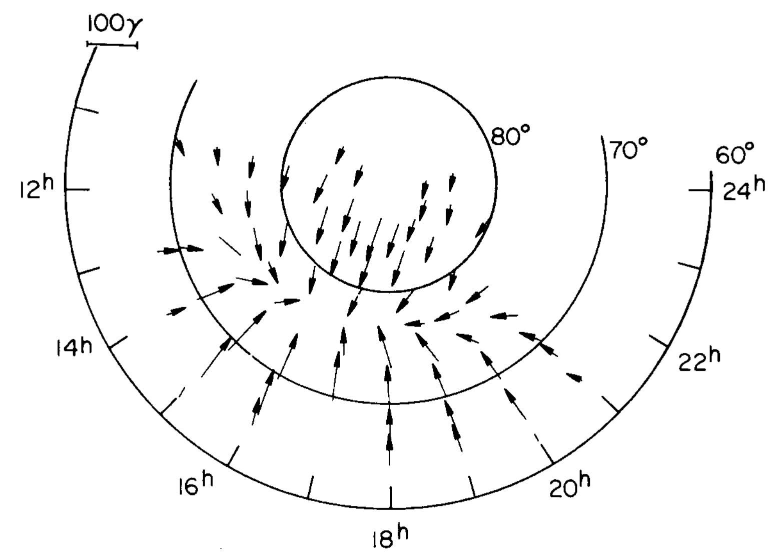

Figure 9. Comparison between the horizontal disturbance at the earth's surface due to HLS and the measured horizontal disturbance at the earth's surface for geomagnetic summer, Kp = 2^- to 3^+ and Toward interplanetary magnetic sectors. Coordinates are MLT and invariant latitude.

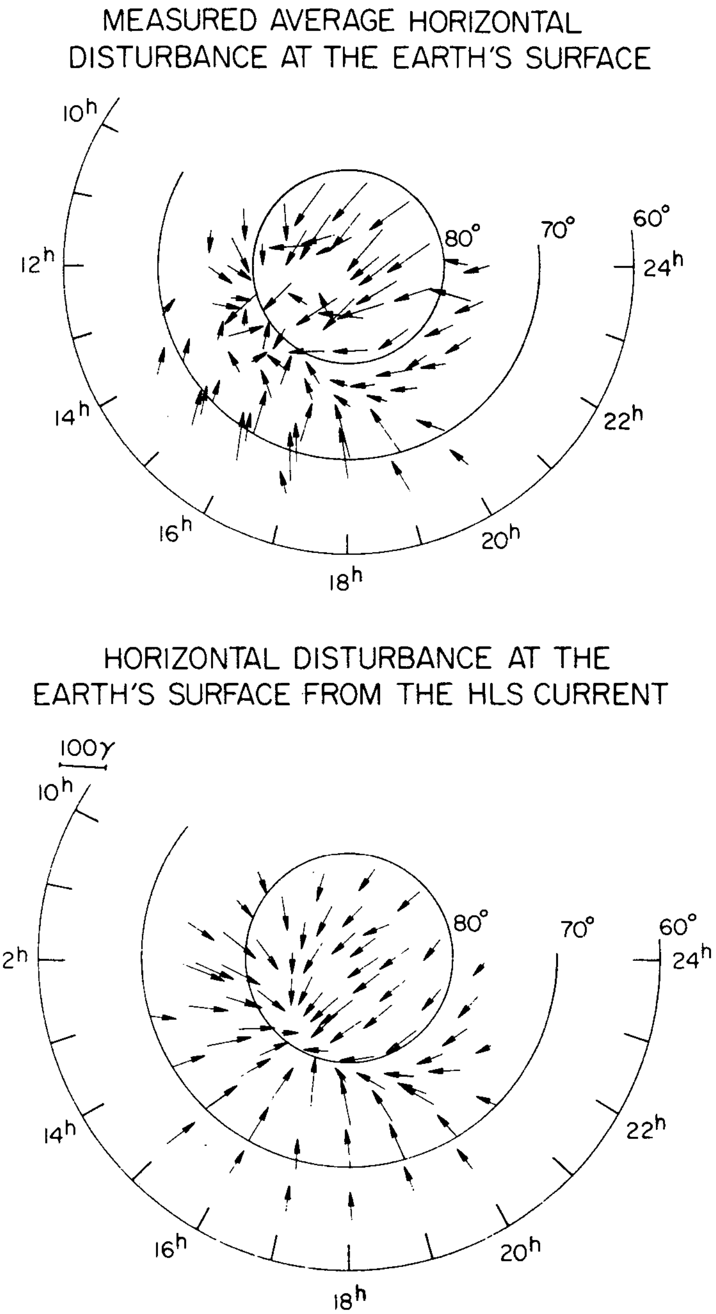

Figure 10. Comparison between the horizontal disturbance at the earth's surface due to HLS and the measured horizontal disturbance at the earth's surface for geomagnetic summer, Kp = 2^- to 3^+ and Away interplanetary magnetic sectors. Coordinates are MLT and invariant latitude.

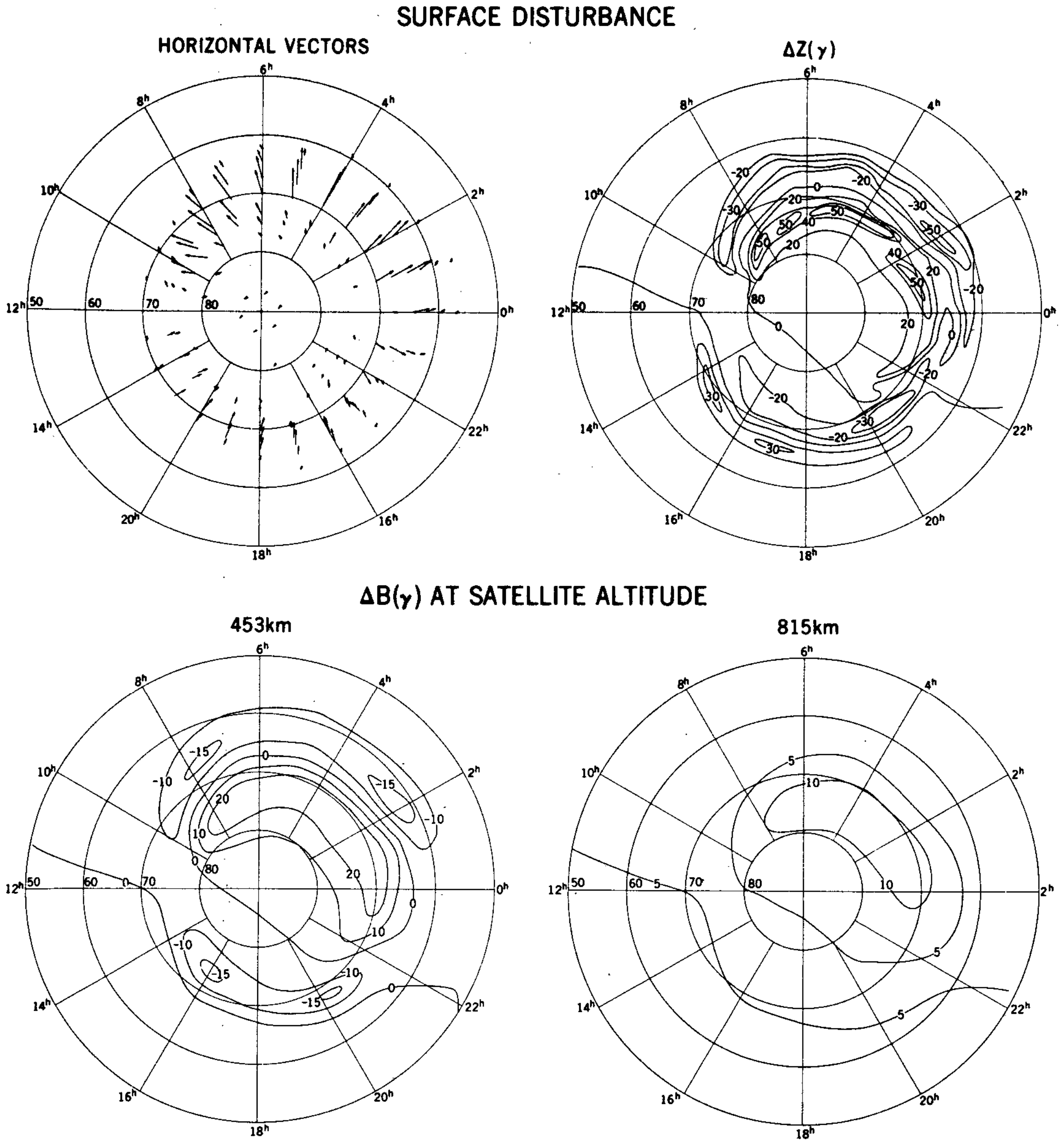

Figure 11. Magnetic disturbance from model electrojet. Coordinates are MLT and invariant latitude. The scale for the horizontal vectors is 200γ for a 10° displacement in latitude.

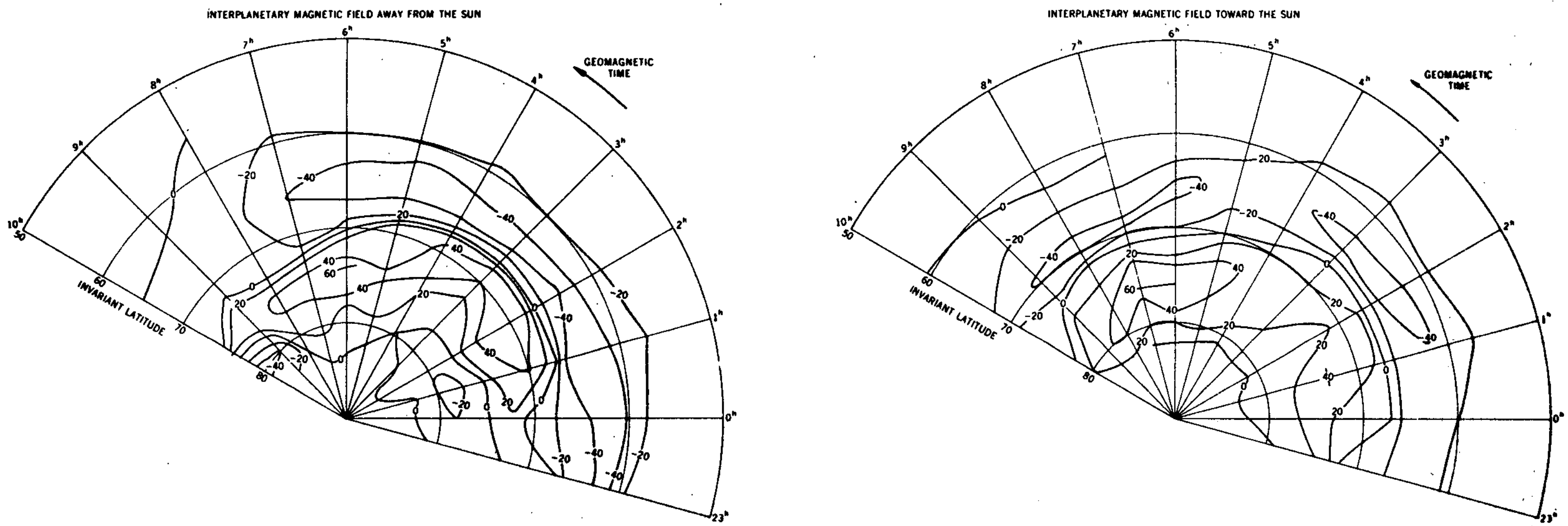

Figure 12. Measured surface ΔZ (γ) **minus average** ΔB at 700-900 km altitude. Kp = 2^- to 3^+, geomagnetic equinox.

OGO-4 POLAR PLOT

9/21/67, NORTH
GEOMAGNETIC COORDINATES

SURFACE MAGNETIC FIELD MEASUREMENTS

ARROW INDICATES TIME OF SATELLITE PASS

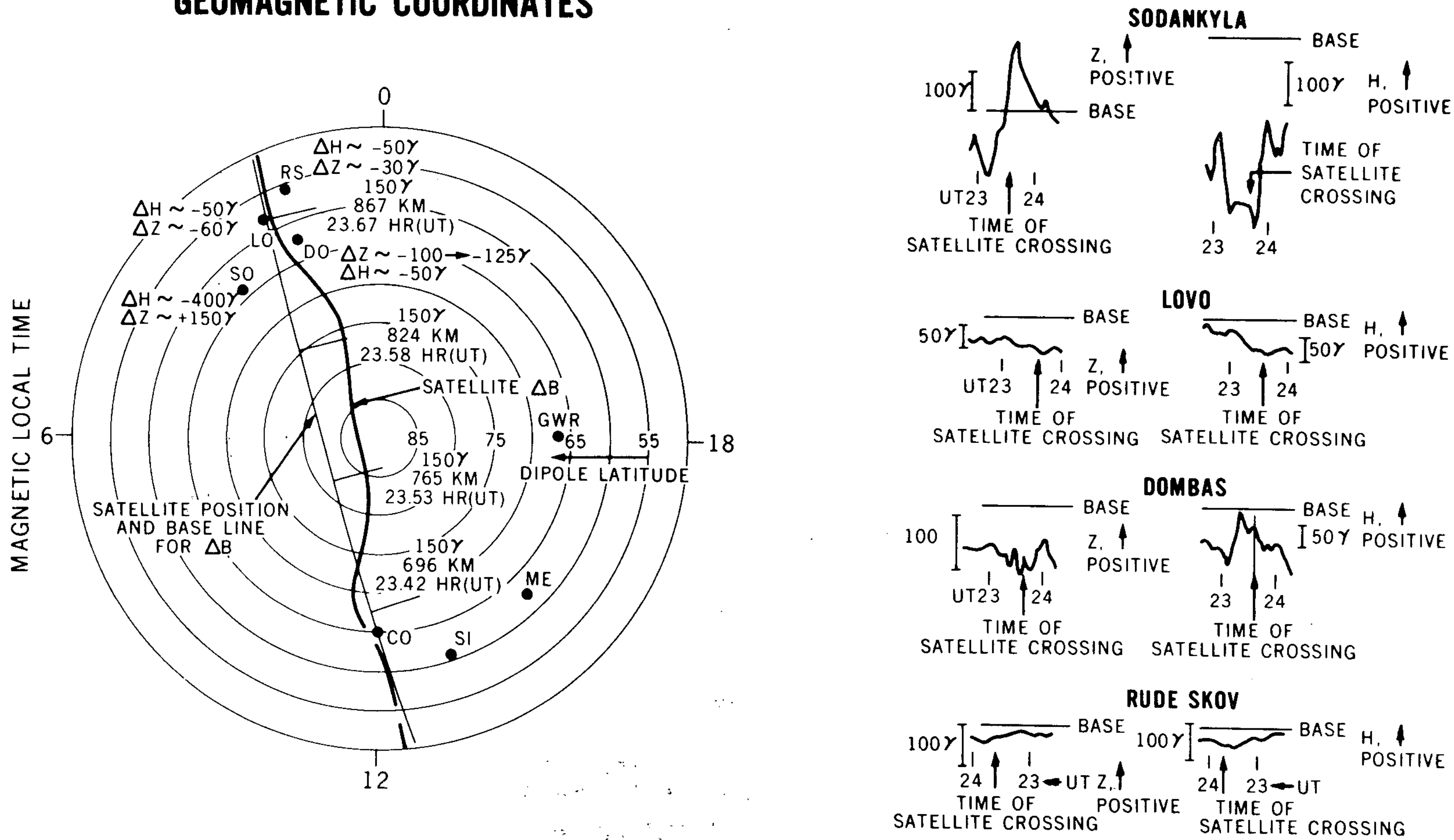

Figure 13

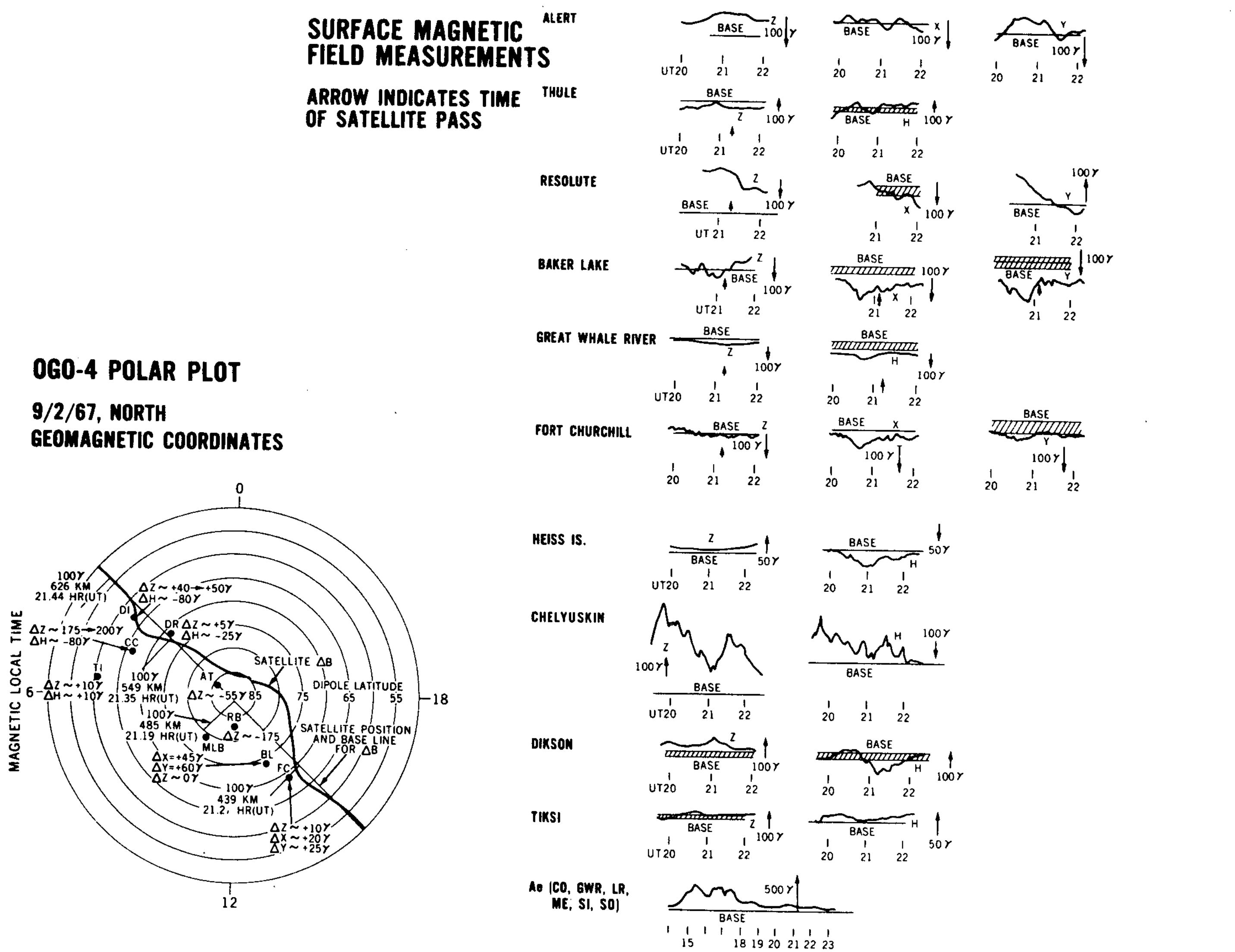

SURFACE MAGNETIC FIELD MEASUREMENTS
ARROW INDICATES TIME OF SATELLITE PASS
ALERT
THULE
RESOLUTE
BAKER LAKE
GREAT WHALE RIVER
FORT CHURCHILL
HEISS IS.
CHELYUSKIN
DIKSON
TIKSI
Ae (CO, GWR, LR, ME, SI, SO)
BASE
OGO-4 POLAR PLOT
9/2/67, NORTH
GEOMAGNETIC COORDINATES
MAGNETIC LOCAL TIME
SATELLITE ΔB
DIPOLE LATITUDE
SATELLITE POSITION AND BASE LINE FOR ΔB
0
6
12
18

Figure 14

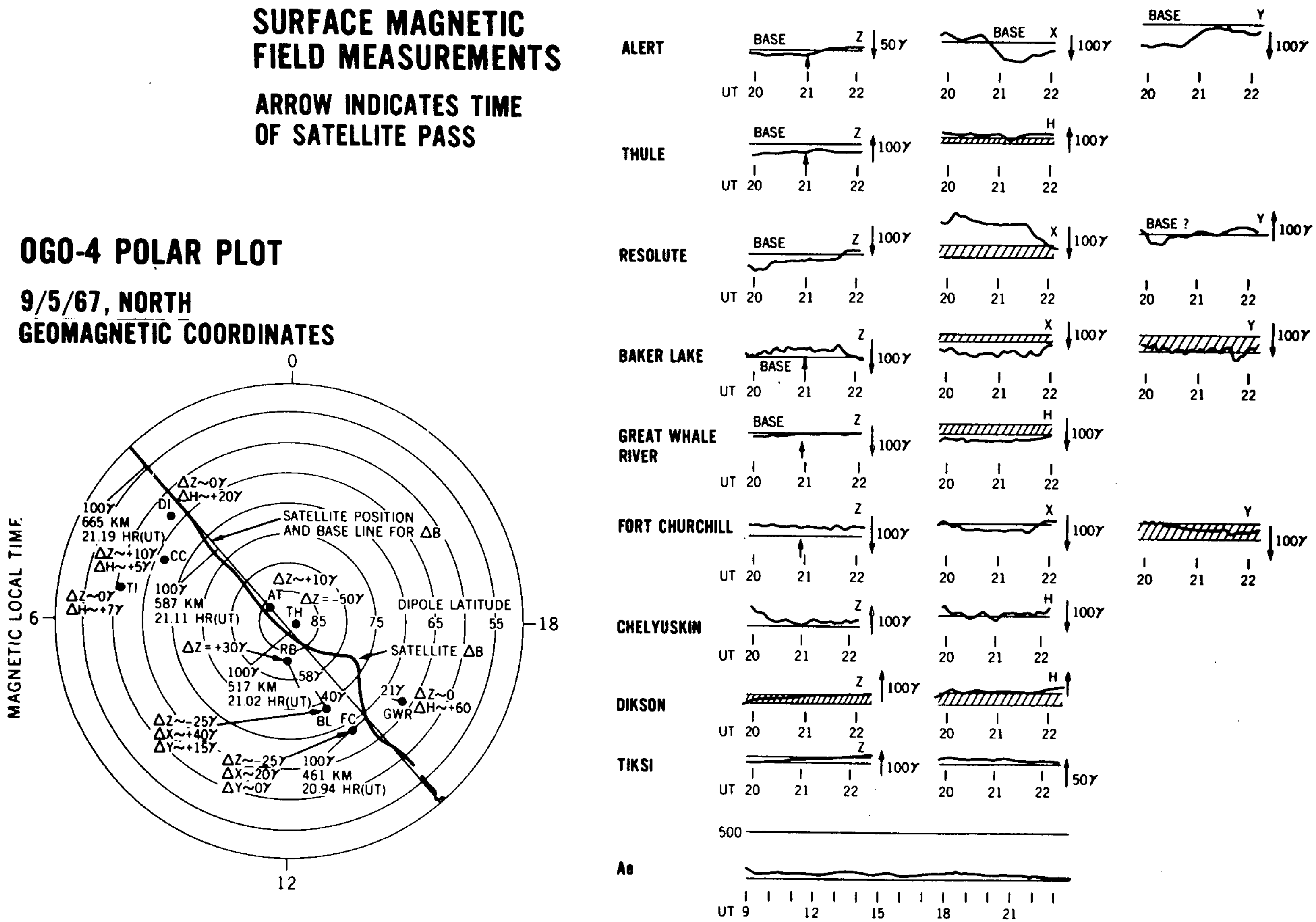
SURFACE MAGNETIC FIELD MEASUREMENTS
ARROW INDICATES TIME OF SATELLITE PASS
OGO-4 POLAR PLOT
9/5/67, NORTH
GEOMAGNETIC COORDINATES
MAGNETIC LOCAL TIME
0
6
12
18
SATELLITE POSITION AND BASE LINE FOR ΔB
SATELLITE ΔB
DIPOLE LATITUDE
85
75
65
55
DI
CC
TI
AT
TH
RB
BL
FC
GWR
ΔZ~0γ
ΔH~+20γ
100γ
665 KM
21.19 HR(UT)
ΔZ~+10γ
ΔH~+5γ
ΔZ~0γ
ΔH~+7γ
100γ
587 KM
21.11 HR(UT)
ΔZ~+10γ
ΔZ = -50γ
ΔZ = +30γ
100γ
517 KM
21.02 HR(UT)
58γ
40γ
21γ
ΔZ~0
ΔH~+60
ΔZ~-25γ
ΔX~+40γ
ΔY~+15γ
ΔZ~-25γ
ΔX~20γ
ΔY~0γ
100γ
461 KM
20.94 HR(UT)
ALERT
THULE
RESOLUTE
BAKER LAKE
GREAT WHALE RIVER
FORT CHURCHILL
CHELYUSKIN
DIKSON
TIKSI
Ae
BASE
BASE ?
Z
X
Y
H
50γ
100γ
500
UT 20 21 22
UT 9 12 15 18 21

Figure 15

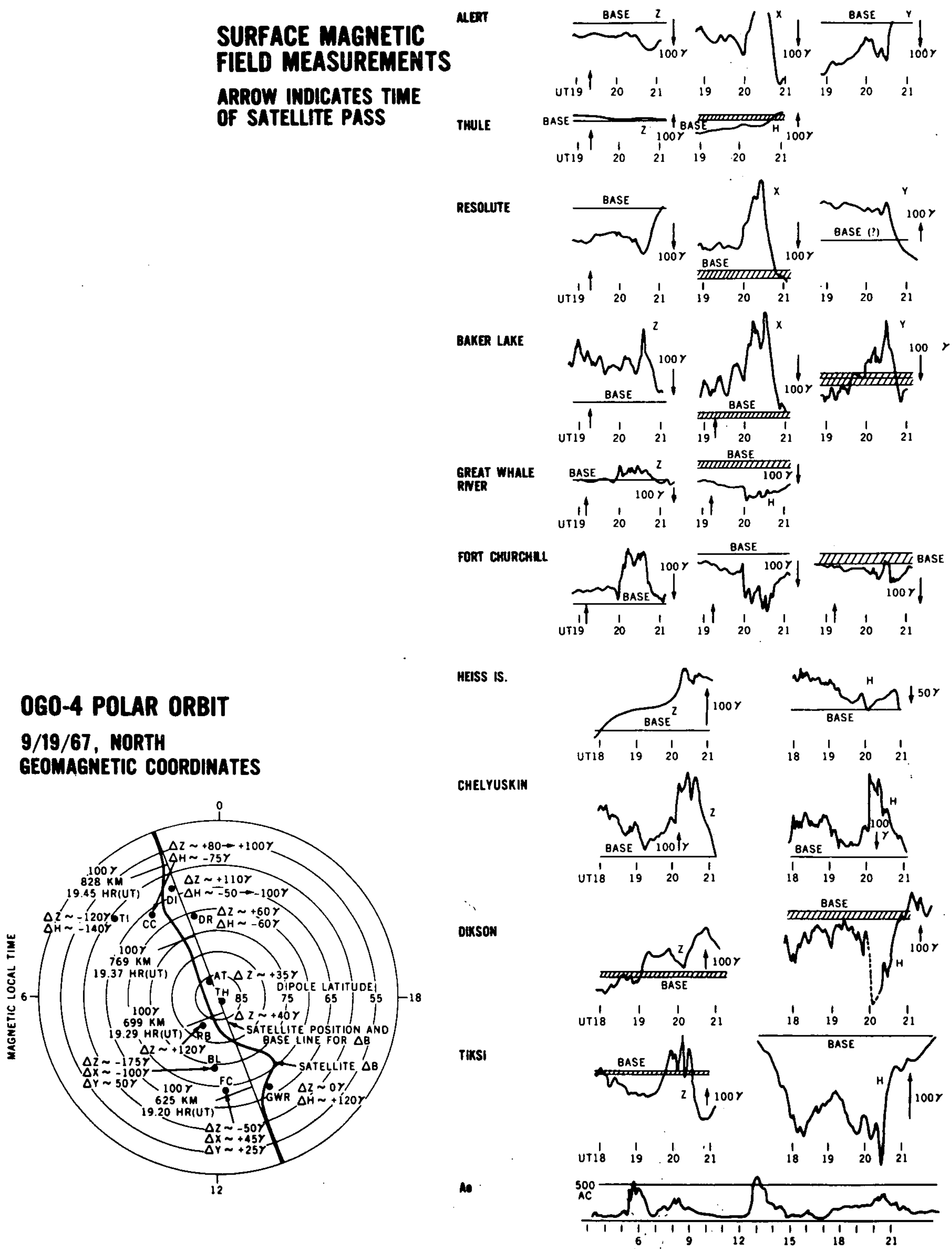
SURFACE MAGNETIC FIELD MEASUREMENTS
ARROW INDICATES TIME OF SATELLITE PASS
ALERT
THULE
RESOLUTE
BAKER LAKE
GREAT WHALE RIVER
FORT CHURCHILL
HEISS IS.
CHELYUSKIN
DIKSON
TIKSI
Ae
BASE
100γ
50γ
UT19
UT18
500 AC
OGO-4 POLAR ORBIT
9/19/67, NORTH
GEOMAGNETIC COORDINATES
MAGNETIC LOCAL TIME
DIPOLE LATITUDE
SATELLITE POSITION AND BASE LINE FOR ΔB
SATELLITE ΔB
100γ
828 KM
19.45 HR(UT)
769 KM
19.37 HR(UT)
699 KM
19.29 HR(UT)
625 KM
19.20 HR(UT)

Figure 16

CORRELATION OF POLAR ACTIVITY WITH AE INDEX

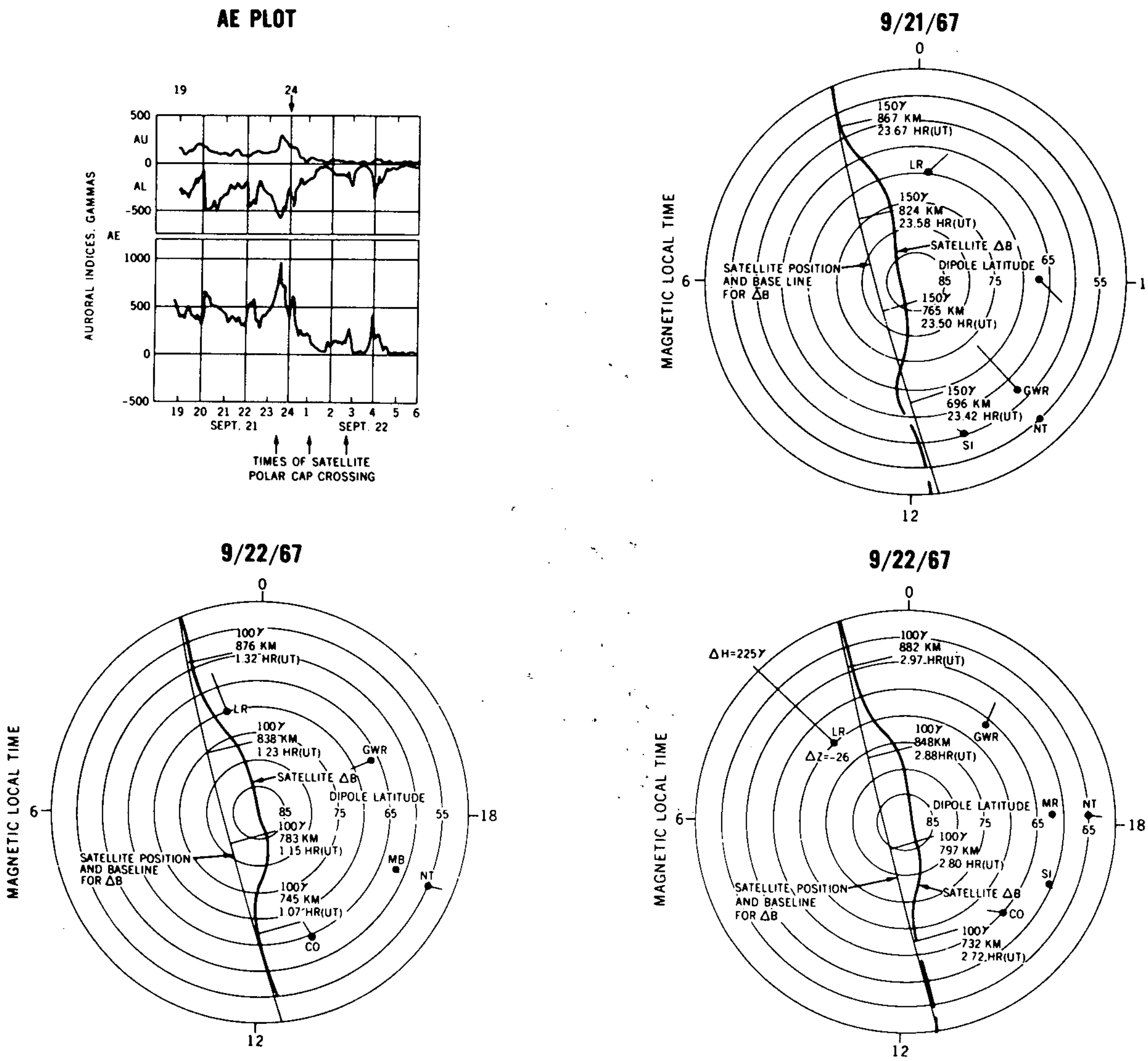

Figure 17

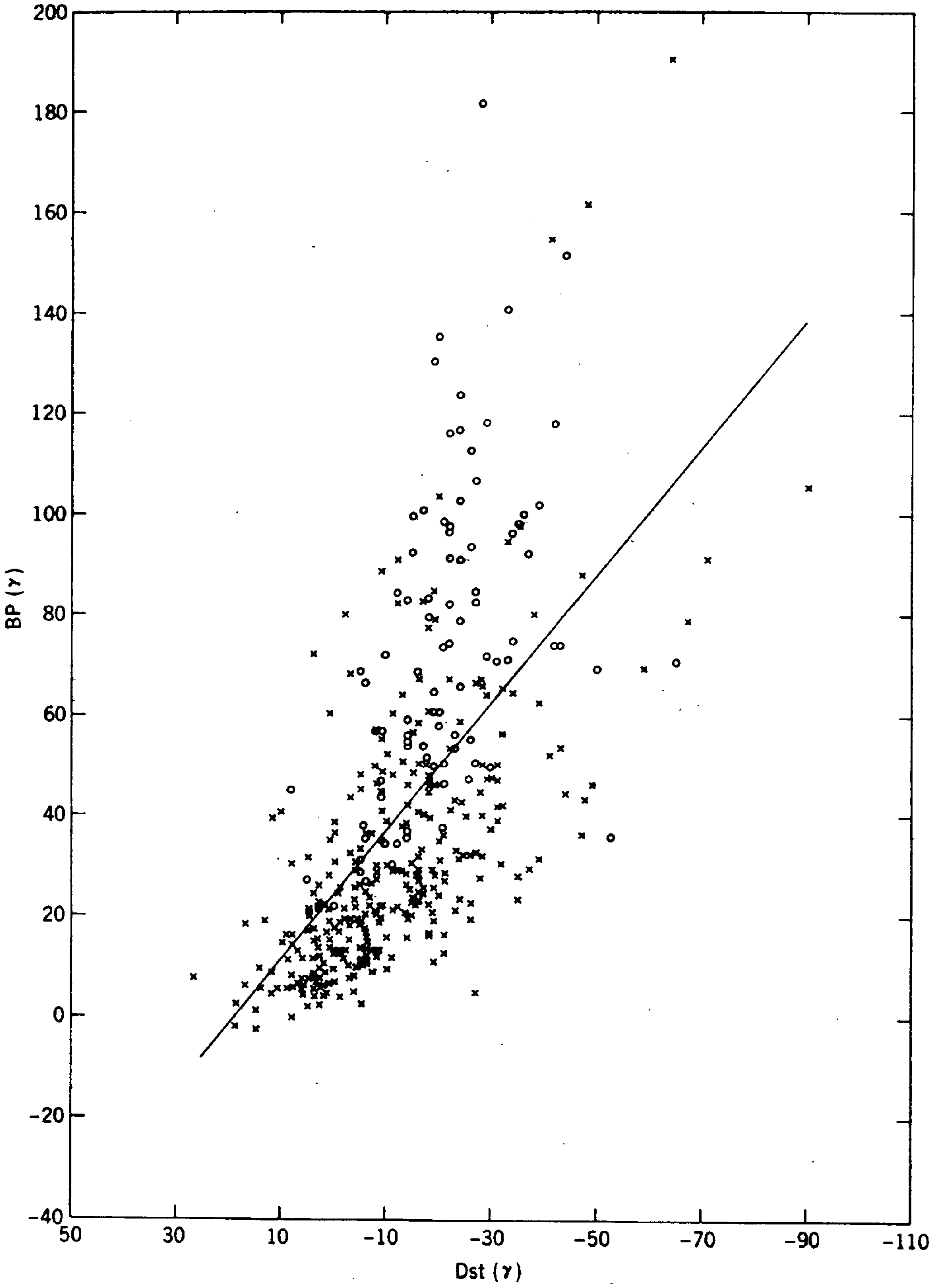

Figure 18. Bp vs Dst. BP is the maximum ΔB from individual passes over the polar cap between 2-5^h MLT. All data is for Kp $\leqslant 4^-$, altitude >700 km. x means the AL index is greater than -150γ, o means that AL is less than -150γ.

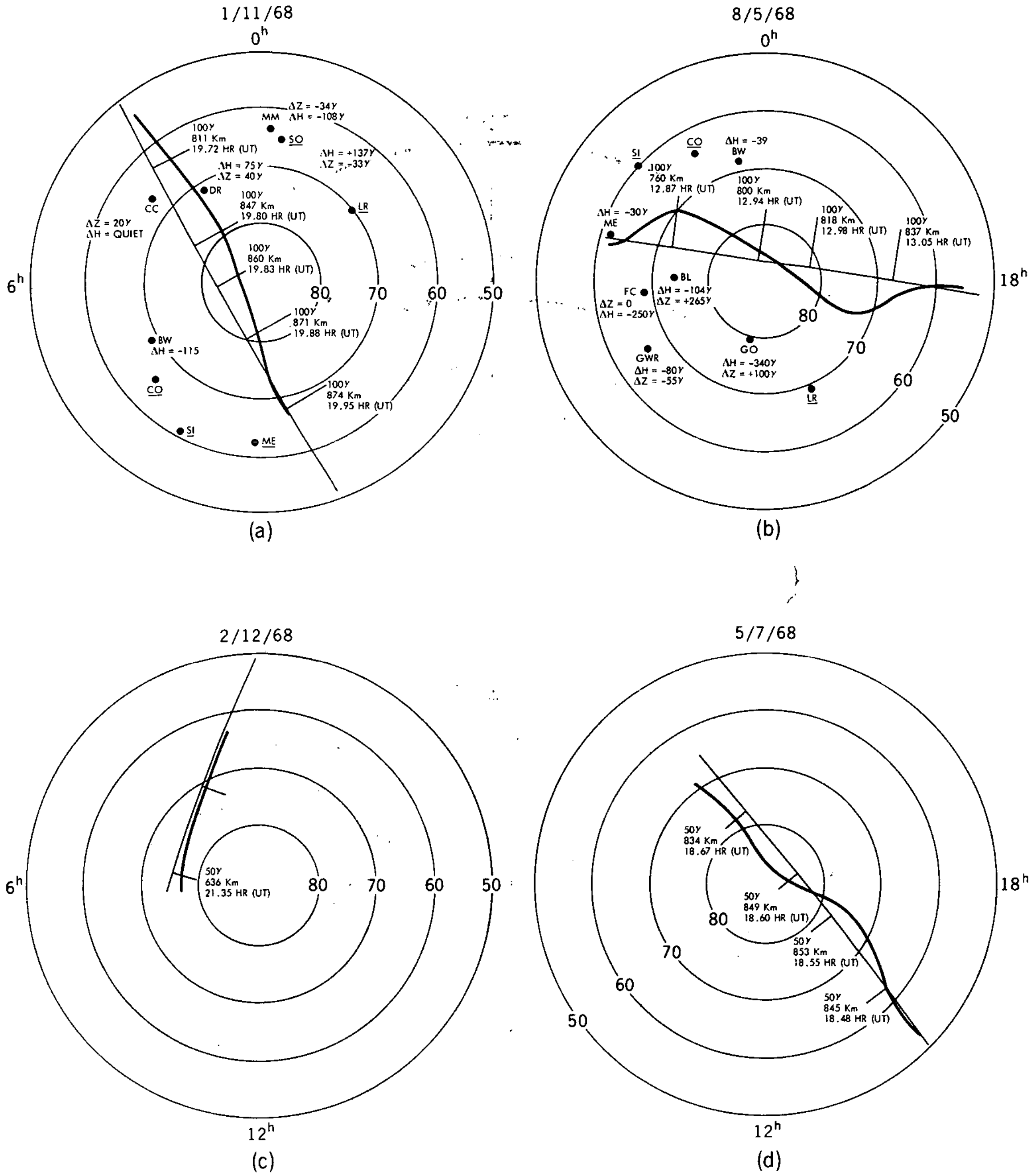

Figure 19. Example of OGO-6 data, northern hemisphere, where the positive ΔB differs from that expected from the ECS and westward electrojet.

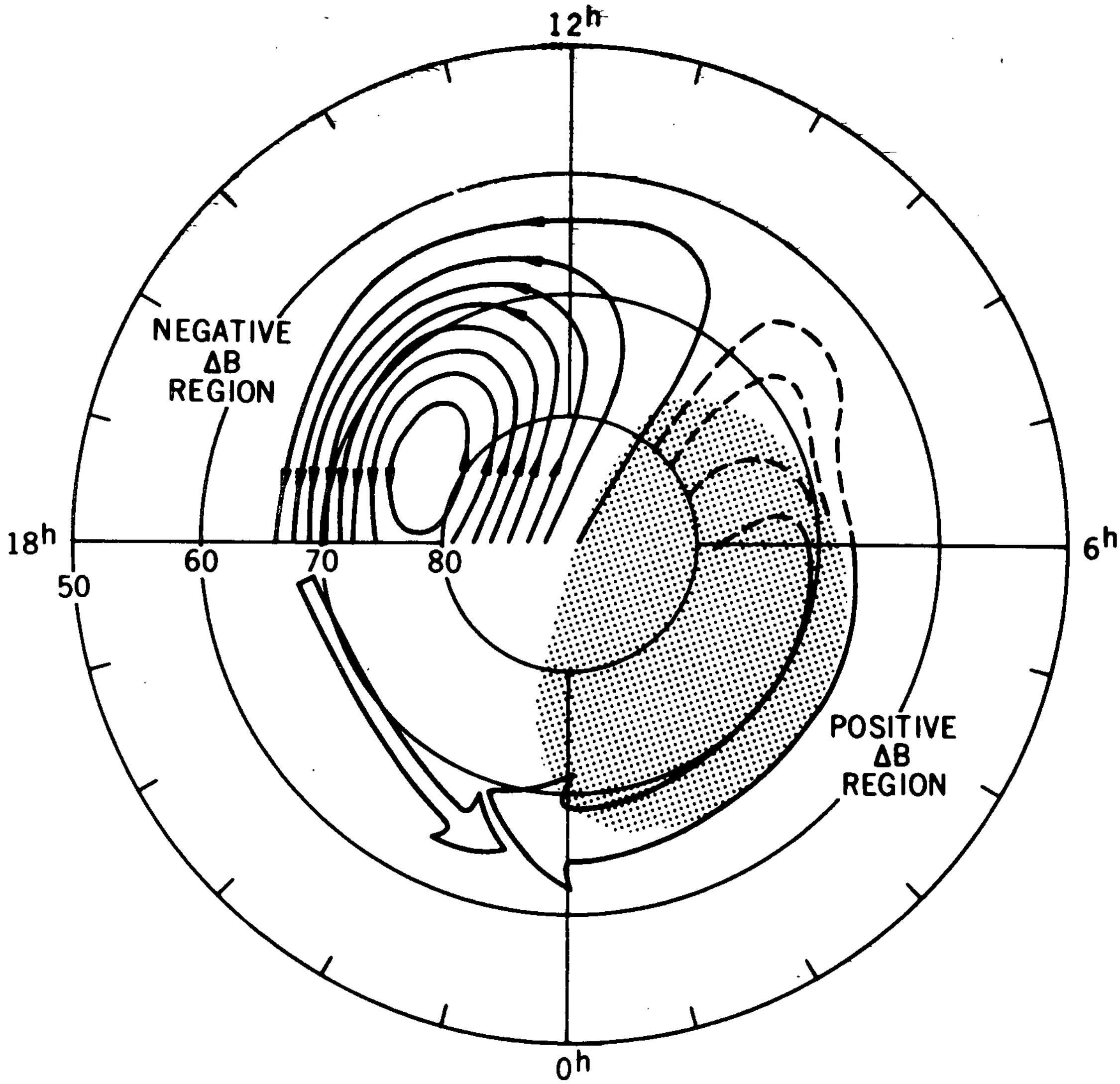

Figure 20. Conceptual drawing of proposed ionospheric source currents. The positive ΔB region is shaded. A probable additional source is the Equatorial Current Sheet.

NASA–GSFC